Search for new physics in the final state with a single photon and large missing transverse momentum in proton-proton collisions at $\sqrt{s} = 13$ TeV

A. Hayrapetyan *et al.*[*]
(CMS Collaboration)

(Received 21 November 2025; accepted 12 March 2026; published 30 April 2026)

A search for new physics in events featuring a single photon and missing transverse momentum is presented, using proton-proton $\sqrt{s} = 13$ TeV collision data corresponding to an integrated luminosity of 101 fb^{-1} collected by the CMS experiment at the CERN LHC between 2017 and 2018. This analysis, combined with a previous study of 36 fb^{-1} of 2016 data (totaling 137 fb^{-1}), reveals no significant deviations from standard model expectations. The results are then used to establish 95% confidence level limits on parameters in theoretical models involving dark matter and large extra dimensions. Compared to the 2016-only analysis, this search achieves up to a 14% improvement in exclusion reach for mediator masses in simplified dark matter models, along with 11% and 10% enhancements in the limits on the effective field theory suppression scale and the fundamental Planck scale, respectively. These results are the most stringent constraints on these parameters to date.

DOI: 10.1103/f9r8-styj

I. INTRODUCTION

This paper details a search by the CMS experiment at the CERN LHC for a distinctive signature of new physics: events with a high-energy photon and a substantial imbalance in transverse momentum. This "monophoton" final state serves as a crucial probe for various theoretical scenarios, including those that feature large extra dimensions or contain dark matter (DM).

The Arkani-Hamed, Dimopoulos, and Dvali (ADD) model [1–3] postulates the existence of a number of large, compactified extra spatial dimensions (n). This framework addresses the hierarchy problem by introducing a lower fundamental Planck scale (M_{D}) in the higher dimensional space, while the effective Planck scale (M_{Pl}) observed in our three-dimensional space is much larger due to propagation of gravity into the extra dimension. This lowering of the Planck scale allows for the potential production of Kaluza-Klein (KK) gravitons. The ADD model predicts the production of a photon and one or more noninteracting KK gravitons(G) via $q\bar{q} \to \gamma G$, as shown in Fig. 1 (left), where each graviton has a mass up to M_{D}. The undetected gravitons result in a significant missing transverse momentum ($p_{\mathrm{T}}^{\mathrm{miss}}$) in the detector.

At the LHC, DM particles are expected to be produced in high-energy collisions and detected indirectly through their interactions with standard model (SM) particles. Since DM is expected to be weakly interacting and invisible to the detectors, these searches typically look for $p_{\mathrm{T}}^{\mathrm{miss}}$ in association with SM particles [4–6]. Simplified models recommended by Ref. [7] are employed to interpret these signatures. These models provide extensions to the SM by introducing a DM particle and a heavy mediator, as shown in Fig. 1 (center). The mediator can be either a vector or an axial vector boson. It couples to the incoming quark through a coupling constant $g_q = 0.25$, and to DM particles with coupling constant $g_{\mathrm{DM}} = 1.0$, with coupling to leptons, g_l, fixed to zero [8]. These coupling values are chosen to ensure that the mediator remains within the narrow-width approximation, where the mediator width is small compared to its mass. This approximation allows the mediator to be treated as a short-lived particle with a well-defined mass, ensuring that the signal modeling remains valid and enabling consistent comparisons across different experimental searches.

The DM particles can also be produced through effective operators involving photons. This interaction is known as the electroweak dark matter (EW-DM) contact interaction and is characterized by the process $q\bar{q} \to Z/\gamma* \to \gamma\chi\bar{\chi}$ [9], where χ is the DM particle, as shown in Fig. 1 (right). This interaction is parametrized by two dimensionless couplings, k_1 and k_2, which control the relative strength of the DM interaction with the EW gauge bosons. The constants k_1 and k_2 are the couplings to the $U(1)_Y$ and $SU(2)_L$ gauge bosons, respectively. The overall interaction

[*]Full author list given at the end of the article.

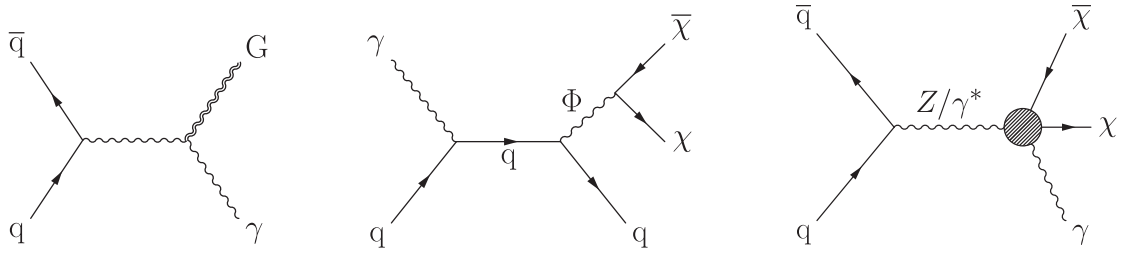

FIG. 1. Leading-order diagrams of graviton production in the ADD model (left), simplified DM model (center), and EW–DM effective interaction (right), with a final state comprising a photon and large $p_{\mathrm{T}}^{\mathrm{miss}}$. Particles χ and $\bar{\chi}$ are the DM and its antiparticle, and Φ in the simplified DM model represents a vector or axial-vector mediator.

is suppressed by a parameter Λ, such that the effective coupling scales as k_1/Λ and k_2/Λ. The parameters defined in these models are the same as those described in a previous CMS search analyzing 2016 data [10].

The analysis targets events with a single high-energy photon and significant $p_{\mathrm{T}}^{\mathrm{miss}}$, a characteristic signature of several new physics scenarios. The dominant SM backgrounds include $Z(\to \nu\bar{\nu}) + \gamma$, $W(\to \ell\bar{\nu}) + \gamma$, and $\gamma +$ jets processes, while other minor background contributions are $Z(\to \ell\bar{\ell}) + \gamma$, $\gamma\gamma$, $t\gamma$, $t\bar{t}\gamma$, $VV\gamma$ (where V refers to a W or Z boson), and beam halo events.

A similar search in pp collisions at $\sqrt{s} = 13$ TeV, based on a dataset corresponding to an integrated luminosity of 139 fb^{-1}, has been reported by the ATLAS experiment [11]. No significant excess over the SM prediction was observed. In that search, the observed lower limit on the axial-vector (vector) mediator mass was determined to be 1460 (1470) GeV for low DM masses, assuming the same g_q, g_{DM}, and g_l coupling values.

While the ATLAS search focuses solely on simplified models for DM, the CMS search also explores the ADD model of large extra dimensions and the EW-DM framework. The previous search in the same final state by the CMS experiment [10] was based on data collected during 2016 corresponding to an integrated luminosity of 36 fb^{-1}. In this paper, we analyze 2017 and 2018 data, and combine with the previously published result using 2016 data [10]. The combined dataset corresponds to a total integrated luminosity of 137 fb^{-1}. The results presented here supersede those of the previous search.

The structure of this paper is as follows. Section II provides a description of the CMS detector apparatus, along with the algorithm employed to reconstruct particles in pp collision events within the detector. Section III outlines the criteria that events must meet to be included in the signal region (SR) and control region (CR). Section IV lists the generators used to model signal and background processes. Section V describes the methods used to estimate the expected background yields in the SR and CR. Systematic uncertainties are discussed in Sec. VI. The results and interpretations are presented in Sec. VII, and the overall conclusions are summarized in Sec. VIII. The tabulated results are also provided in the HEPData record [12].

II. THE CMS DETECTOR AND EVENT RECONSTRUCTION

The CMS apparatus [13,14] is a multipurpose, nearly hermetic detector, designed to trigger on and identify electrons, muons, photons, and charged and neutral hadrons [15–17]. Its central feature is a superconducting solenoid of 6 m internal diameter, providing a magnetic field of 3.8 T. Within the solenoid volume are a silicon pixel and strip tracker, a lead tungstate crystal electromagnetic calorimeter (ECAL), and a brass and scintillator hadron calorimeter (HCAL), each composed of a barrel and two endcap sections. Forward calorimeters extend the pseudorapidity coverage provided by the barrel and end cap detectors. Muons within the pseudorapidity range $|\eta| < 2.4$ are reconstructed using gas-ionization detectors embedded in the steel flux-return yoke outside the solenoid. More detailed descriptions of the CMS detector, together with a definition of the coordinate system used and the relevant kinematic variables, can be found in Refs. [13,14].

Events of interest are selected in real time using a two-tiered trigger system. The first level, composed of custom hardware processors, uses information from the calorimeters and muon detectors to select events at a rate of around 100 kHz within a fixed latency of about 4 μs [18]. The second level, known as the high-level trigger, consists of a farm of processors running a version of the full event reconstruction software optimized for fast processing, and reduces the event rate to approximately 1 kHz before data storage [19,20].

The primary vertex is taken to be the vertex corresponding to the hardest scattering in an event, evaluated using tracking information alone, as described in Sec. 9.4.1 of Ref. [21]. The global event reconstruction (also called particle-flow (PF) event reconstruction [22]) aims to reconstruct and identify each individual particle in an event, with an optimized combination of all subdetector information. In this process, the identification of the particle type (photon, electron, muon, charged hadron, neutral hadron) plays an important role in the determination

of the particle direction and energy. Photons are identified as ECAL energy clusters not linked to the extrapolation of any charged-particle trajectory to the ECAL. Electrons are identified as a primary charged-particle track and potentially many ECAL energy clusters corresponding to the extrapolation of this track to the ECAL and to possible bremsstrahlung photons emitted along the way through the tracker material. Muons are identified as tracks in the central tracker consistent with either a track or several hits in the muon system, and associated with calorimeter deposits compatible with the muon hypothesis. Charged hadrons are identified as charged-particle tracks that are identified neither as electrons nor as muons. Finally, neutral hadrons are identified as HCAL energy clusters not linked to any charged-hadron trajectory, or as a combined ECAL and HCAL energy excess with respect to the expected charged-hadron energy deposit.

The energy of photons is obtained from the ECAL measurement. The energy of electrons is determined from a combination of the track momentum at the main interaction vertex, the associated ECAL cluster energy, and the energy sum of all bremsstrahlung photons attached to the track. Muon energy is determined from the track momentum. The energy of charged hadrons is determined from a combination of the track momentum and the corresponding ECAL and HCAL energies, corrected for the response function of the calorimeters to hadronic showers. Finally, the energy of neutral hadrons is obtained from the corrected ECAL and HCAL energies associated with those particles. For each event, hadronic jets are clustered from these reconstructed particles using the infrared and collinear safe anti-k_{T} algorithm [23,24] with a distance parameter of 0.4. Jet momentum is determined as the vectorial sum of all particle momenta in the jet, and is found from simulation to be, on average, within 5% to 10% of the true momentum over the entire p_{T} spectrum and detector acceptance. Additional pp interactions within the same or nearby bunch crossings (pileup) can contribute additional tracks and calorimetric energy depositions to the jet momentum. To mitigate this effect, charged-particles identified as originating from pileup vertices are discarded, and an offset correction is applied to correct for remaining contributions [25].

Jet energy corrections are derived from simulation to bring the measured detector response of jets to that of particle-level jets on average. In situ measurements of the momentum balance in dijet, $\gamma+\mathrm{jet}$, $Z+\mathrm{jet}$, and multijet events are used to account for any residual differences in the jet energy scale between data and simulation [25]. The jet energy resolution amounts typically to 15%–20% at 30 GeV, 10% at 100 GeV, and 5% at 1 TeV [25]. Additional selection criteria are applied to each jet to suppress jets with anomalous energy deposits, noise, or reconstruction failures in specific subdetector components, such as the calorimeters or tracker [26,27].

The missing transverse momentum vector $\vec{p}_{\mathrm{T}}^{\,\mathrm{miss}}$ is computed as the negative vector sum of the transverse momenta of all the PF candidates in an event, and its magnitude is denoted as $p_{\mathrm{T}}^{\mathrm{miss}}$ [26]. The $\vec{p}_{\mathrm{T}}^{\,\mathrm{miss}}$ is modified to account for corrections to the energy scale of the reconstructed jets in the event. Anomalous high-$p_{\mathrm{T}}^{\mathrm{miss}}$ events can arise from a variety of reconstruction failures, detector malfunctions, or noncollision backgrounds. Such events are rejected by event filters that are designed to identify more than 85%–90% of the spurious high-$p_{\mathrm{T}}^{\mathrm{miss}}$ events with a mistagging rate of less than 0.1% [26].

In the barrel section of the ECAL, an energy resolution of approximately 1% is achieved for unconverted or late-converting photons at energies of $\mathcal{O}(10\ \mathrm{GeV})$. The energy resolution of the remaining barrel photons is about 1.3% up to $|\eta|=1$, changing to about 2.5% at $|\eta|=1.4$ [28].

III. EVENT SELECTION

The integrated luminosity of the analyzed data sample is 101.3 fb^{-1}. The data sample was collected using a single-photon trigger that required at least one photon candidate with $p_{\mathrm{T}}>200$ GeV. The trigger efficiency is measured to be about 95% for events passing the analysis selection. Events are selected from the recorded data by requiring $p_{\mathrm{T}}^{\mathrm{miss}}>200$ GeV and the presence of at least one photon with $E_{\mathrm{T}}^{\gamma}>225$ GeV (where E_{T}^{γ} is the transverse energy of the photon) within the fiducial region of the ECAL barrel ($|\eta|<1.44$). The analysis is restricted to the barrel region due to its superior energy resolution and lower background contamination compared to the end caps, as well as the limited expected signal contribution in the end cap region. The final sample contains no events with more than one photon meeting the selection criteria.

Photon candidates are identified using calorimetric information, isolation, and the absence of an electron seed. The first two criteria help distinguish genuine photon candidates from electromagnetic (EM) showers originating from hadrons, while the third criterion ensures the photon candidates are not misidentified electrons. The calorimetric requirements for photons consist of the ratio of energy deposited in the HCAL to that in the ECAL ($H/E<0.023$) and $\sigma_{i\eta i\eta}<0.0103$. The variable $\sigma_{i\eta i\eta}$, described in detail in Ref. [28], represents the width of the EM shower in the η direction, which is generally larger in showers from hadronic activity. For a photon candidate to be considered as isolated, the scalar sums of the transverse momenta of charged hadrons, neutral hadrons, and photons within a cone of $\Delta R=\sqrt{(\Delta\eta)^2+(\Delta\phi)^2}<0.3$ around the candidate photon must fall below a set of corresponding bounds chosen to give 80% signal efficiency. Only the PF candidates that do not overlap with the EM shower of the candidate photon are included in the isolation sums. The charged hadron isolation (I_{ch}) is defined as the scalar sum of the p_{T} of charged hadrons within the cone. The neutral

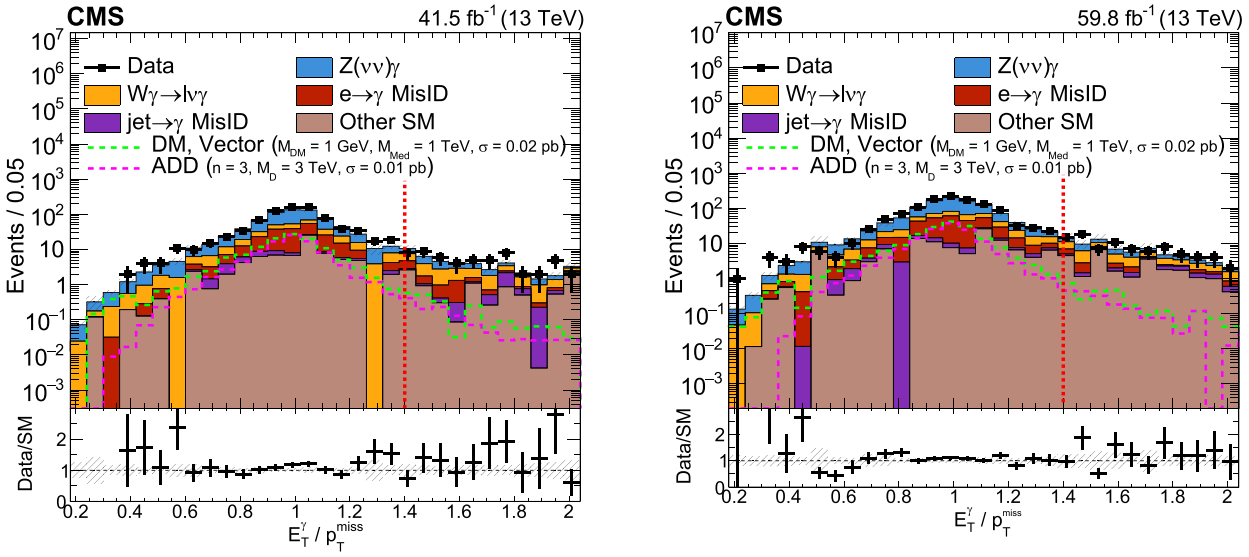

FIG. 2. Distribution of $E_{\mathrm{T}}^{\gamma}/p_{\mathrm{T}}^{\mathrm{miss}}$ for the 2017 (left) and 2018 (right) datasets. Templates for signal hypotheses are shown overlaid as light green and magenta dashed lines along with their cross section values. The cross hatched band represents the total systematic and statistical uncertainties. Events to the right of the red dashed vertical line are excluded.

hadron isolation (I_{nh}) is the scalar sum of the p_{T} of neutral hadrons within the cone, and the photon isolation (I_{ph}) is the sum of p_{T} of photons within the cone, excluding the photon itself. Ideally, the isolation sum over PF charged hadrons should be computed using only the candidates sharing an interaction vertex with the photon candidate. However, because photon candidates are not reconstructed from tracks, their vertex association is undefined. When an incorrect vertex is assigned, nonisolated photon candidates can appear isolated. To reduce the rate for accepting nonisolated photon candidates, the maximum charged-hadron isolation ($I_{\mathrm{ch}}^{\mathrm{max}}$) value over all vertex hypotheses (worst isolation) is used. The above criteria select efficiently both unconverted photons and photons undergoing conversion in the detector material in front of the ECAL.

Stray ECAL clusters produced by mechanisms other than pp collisions can be misidentified as photons. Beam halo muons in particular, which accompany the proton beams and traverse the detector longitudinally, contribute significantly to the rate of false photon candidates. To reject this background, the maximum of the total calorimeter energy summed along all possible paths of beam halo particles passing through the cluster (halo total energy), calculated for each photon candidate, must be below 4.9 GeV. To better constrain this background, the signal region is split into two parts based on the azimuthal angle ϕ of the photon. The region with $|\phi| < 0.5$ is called the horizontal region, and the rest is called the vertical region. This helps in improving the estimation of the beam halo contribution, as discussed later in Sec. V D.

Events with a high-p_{T} photon and large $p_{\mathrm{T}}^{\mathrm{miss}}$ are subjected to further requirements to suppress SM background processes that feature a genuine high-energy photon, but not a significant amount of $p_{\mathrm{T}}^{\mathrm{miss}}$. One such SM process is $\gamma+$jets, where an apparent large $p_{\mathrm{T}}^{\mathrm{miss}}$ is often the result of a mismeasured jet energy. In contrast to signal processes, $p_{\mathrm{T}}^{\mathrm{miss}}$ is typically smaller than E_{T}^{γ} in these events, so requiring the ratio of E_{T}^{γ} to $p_{\mathrm{T}}^{\mathrm{miss}}$ to be less than 1.4 effectively rejects 63% of the $\gamma+$jets background while retaining 99% of the signal efficiency. Figure 2 shows the comparison of the observed and simulated $E_{\mathrm{T}}^{\gamma}/p_{\mathrm{T}}^{\mathrm{miss}}$ distribution.

Events are also rejected if the minimum opening angle between $\vec{p}_{\mathrm{T}}^{\mathrm{miss}}$ and the direction of any of the (up to four) highest-p_{T} jets, $\min\Delta\phi(\vec{p}_{\mathrm{T}}^{\mathrm{miss}}, \vec{p}_{\mathrm{T}}^{\mathrm{jet}})$, is less than 0.5 radians. Only jets with $p_{\mathrm{T}} > 30$ GeV and $|\eta| < 5$ are considered in the $\min\Delta\phi(\vec{p}_{\mathrm{T}}^{\mathrm{miss}}, \vec{p}_{\mathrm{T}}^{\mathrm{jet}})$ calculation. The expected and observed numbers of jets in the SR are small, typically zero or one. For the $\gamma+$jets process, rare and anomalous mismeasurement of E_{T}^{γ} can also lead to large $p_{\mathrm{T}}^{\mathrm{miss}}$. For this reason, the photon candidate transverse momentum vector ($\vec{p}_{\mathrm{T}}^{\gamma}$) and $\vec{p}_{\mathrm{T}}^{\mathrm{miss}}$ must be separated by more than 0.5 radians.

This is illustrated in Fig. 3, which shows the $\Delta\phi(\vec{p}_{T}^{\mathrm{miss}}, \vec{p}_{\mathrm{T}}^{\gamma})$ distribution before any selection on this variable is applied. This requirement effectively suppresses backgrounds from QCD multijet events, electron to photon misidentification and $\gamma+$jets events.

During the 2018 data-taking period, a section of the HCAL was not working, leading to irrecoverable mismeasurement in a localized region of the detector ($-1.57 < \phi < -0.87$, $-3.0 < \eta < -1.3$). To avoid contamination from such mismeasurement, events containing any jet with $p_{\mathrm{T}} > 30$ GeV in this region are rejected.

The SM $W(\to \ell\bar{\nu}) + \gamma$ process is reduced by vetoing events in which an electron or a muon with $p_{\mathrm{T}} > 10$ GeV is

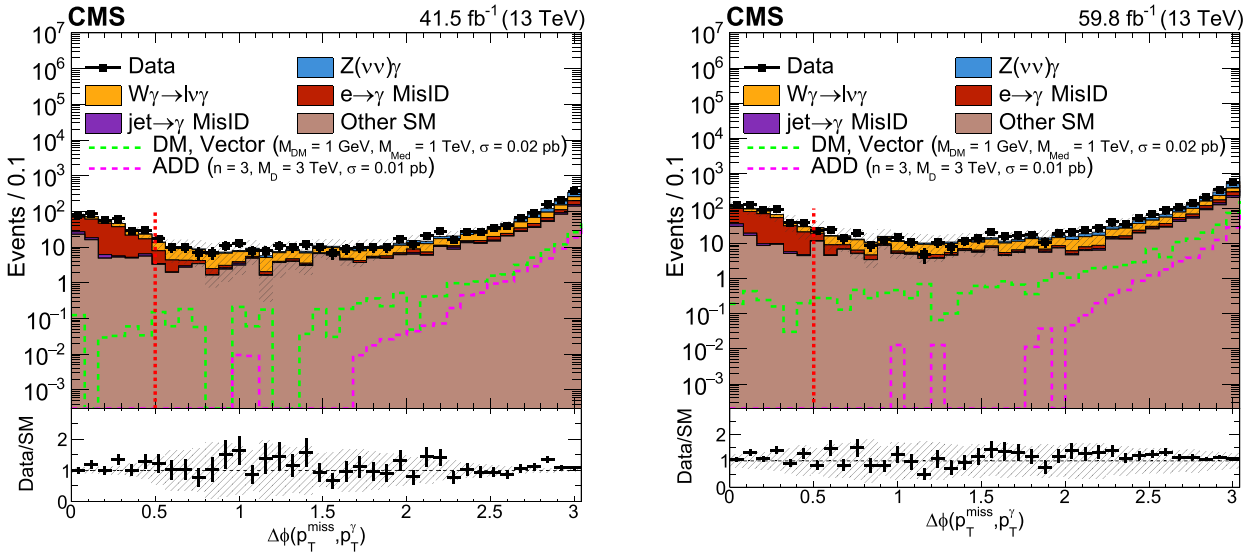

FIG. 3. Distribution of $\Delta\phi(\vec{p}_T^{\,\mathrm{miss}}, \vec{p}_\mathrm{T}^{\,\gamma})$ for the 2017 (left) and 2018 (right) datasets. Templates for signal hypotheses are shown overlaid as light green and magenta dashed lines along with their cross section values. The cross hatched band represents the total systematic and statistical uncertainties. Events to the left of the red dashed vertical line are excluded.

separated from the photon by $\Delta R > 0.5$. Electrons and muons are selected using "loose" identification (ID) criteria that include isolation and other quality requirements [15,29]. The event selection criteria for the SR are summarized in Table I.

To estimate the dominant backgrounds and constrain their normalization in data, several dedicated CRs are defined. The single-lepton CRs (single-electron and single-muon) are designed to constrain the $W(\to \ell\bar{\nu}) + \gamma$ background, while the dilepton CRs (dielectron and dimuon) constrain the yields of $Z(\to \ell\overline{\ell}) + \gamma$ events, which serve as a proxy for the $Z(\to \nu\bar{\nu}) + \gamma$ background.

The single-electron (single-muon) CR is defined by a requirement of exactly one tight electron (muon) with $p_\mathrm{T} > 30$ GeV and $|\eta| < 2.5(2.4)$, in addition to a photon requirement that is identical to the one for the signal region (SR). To suppress the contributions from large-$p_\mathrm{T}^{\mathrm{miss}}$ processes other than $W(\to \ell\bar{\nu}) + \gamma$, the transverse mass $m_T = \sqrt{2p_\mathrm{T}^{\mathrm{miss}} p_\mathrm{T}^{\ell}[1 - \cos\Delta\phi(\vec{p}_\mathrm{T}^{\,\mathrm{miss}}, \vec{p}_\mathrm{T}^{\,\ell})]}$ must be less than 160 GeV, where p_T^{ℓ} denotes the transverse momentum of the selected lepton (electron or muon). Additionally, for the single-electron CR, $p_\mathrm{T}^{\mathrm{miss}}$ must be greater than 50 GeV to limit the contribution from the $\gamma +$ jets process, where a jet is misidentified as an electron. Finally, the recoil vector $\vec{U} = \vec{p}_\mathrm{T}^{\,\mathrm{miss}} + \vec{p}_\mathrm{T}^{\,\ell}$, which serves as this region's analog for $\vec{p}_\mathrm{T}^{\,\mathrm{miss}}$ in the SR, must satisfy identical requirements to those for the $\vec{p}_\mathrm{T}^{\,\mathrm{miss}}$ in the SR.

The dielectron (dimuon) CR is defined by exactly two electrons (muons) of opposite electric charge, in addition to the photon, with $60 < m_{\ell\ell} < 120$ GeV, where $m_{\ell\ell}$ is the invariant mass of the dilepton system. The recoil vector of this region is $\vec{U} = \vec{p}_\mathrm{T}^{\,\mathrm{miss}} + \vec{p}_\mathrm{T}^{\,\ell\ell}$, where the transverse momentum of the dilepton system is given by $\vec{p}_\mathrm{T}^{\,\ell\ell} = \vec{p}_\mathrm{T}^{\,\ell_1} + \vec{p}_\mathrm{T}^{\,\ell_2}$ and must satisfy identical requirements to those for the $\vec{p}_\mathrm{T}^{\,\mathrm{miss}}$ in the SR. The event selection criteria for the CRs are summarized in Table II.

TABLE I. Event selection criteria for the SR. The requirements on the trigger, photon identification, and $\Delta\phi$ are listed.

Category	SR
Trigger	$E_\mathrm{T}^{\gamma} > 200$ GeV
γ requirement	$E_\mathrm{T}^{\gamma} > 225$ GeV, $\lvert\eta\rvert < 1.44$ passing 80% signal efficiency selection: $\sigma_{i\eta i\eta} < 0.0103$, $H/E < 0.023$, $I_{\mathrm{ch}}^{\mathrm{max}} < 2.14$ GeV, $I_{\mathrm{ph}} < 0.17\ \mathrm{GeV} + 0.003E_\mathrm{T}^{\gamma}$, $I_{\mathrm{nh}} < 7.25\ \mathrm{GeV} + 0.01E_\mathrm{T}^{\gamma} + 0.00001(E_\mathrm{T}^{\gamma})^2/\mathrm{GeV}$
$p_\mathrm{T}^{\mathrm{miss}}$ requirement	$p_\mathrm{T}^{\mathrm{miss}} > 200$ GeV
Angular separation	$\Delta\phi(\vec{p}_T^{\,\mathrm{miss}}, \vec{p}_\mathrm{T}^{\,\gamma}) > 0.5$
Jet requirement	$\Delta\phi(\vec{p}_\mathrm{T}^{\,\mathrm{jet}}, \vec{p}_T^{\,\mathrm{miss}}) > 0.5$ (for the leading 4 jets)
$\gamma +$ Jets suppression	$E_\mathrm{T}^{\gamma}/p_\mathrm{T}^{\mathrm{miss}} < 1.4$
Lepton veto	No μ^- or e^- with $p_T > 10$ GeV and passing Loose ID criteria

TABLE II. Event selection in the CRs.

Category	Single Lepton ($W(\to \ell\bar{\nu}) + \gamma$)	Double Lepton ($Z(\to \ell\overline{\ell}) + \gamma$)
Trigger, Photon, $\Delta\phi(\text{jet}, p_{\mathrm{T}}^{\mathrm{miss}})$	Same as SR	Same as SR
Lepton	$p_{\mathrm{T}} > 30$ GeV, passing tight ID requirement	Leading: $p_{\mathrm{T}} > 30$ GeV, passing Tight ID requirement Subleading: $p_{\mathrm{T}} > 10$ GeV, opposite charge, passing loose ID requirement
Recoil (U)	$\lvert U\rvert > 200$ GeV, $\Delta\phi(\vec{p}_{\mathrm{T}}^{\,\gamma}, \vec{U}) > 0.5$	$\lvert U\rvert > 200$ GeV, $\Delta\phi(\vec{p}_{\mathrm{T}}^{\,\gamma}, \vec{U}) > 0.5$
Additional requirements	$m_{\mathrm{T}}(\vec{p}_{\mathrm{T}}^{\,\ell}\, \vec{p}_{\mathrm{T}}^{\,\mathrm{miss}}) < 160$ GeV, $p_{\mathrm{T}}^{\mathrm{miss}} > 50$ GeV [only for $W(e\nu)$]	$60 < m_{\ell\ell} < 120$ GeV

IV. SIMULATED SAMPLES

Simulated predictions for signal and some backgrounds derive from Monte Carlo (MC) samples, with the NNPDF3.1 NNLO [30] parton distribution function (PDF) set and the strong coupling constant value set to $\alpha_S = 0.118$.

The simulated events for the $Z(\to \nu\bar{\nu}) + \gamma$, $Z(\to \ell\overline{\ell}) + \gamma$, and $W(\to \ell\bar{\nu}) + \gamma$ SM processes are generated using the MADGRAPH 5_aMC@NLO generator at LO, with up to two extra partons in the matrix element calculations [31]. These are then normalized to the next-to-LO electroweak (NLO EW) and next-to-NLO quantum chromodynamics (NNLO QCD) cross sections using the correction factors described in Sec. V.

Parton showering and hadronization are modeled by PYTHIA 8.240 [32] with the underlying-event tune CP5 [33]. Multiple simulated minimum bias events are overlaid on the primary interaction to model the distribution of pileup in data. Generated particles are processed through the full GEANT4-based simulation of the CMS detector [34,35].

For the DM signal hypotheses, MADGRAPH 5_aMC@NLO is used to produce MC simulated samples at NLO in QCD, requiring $E_{\mathrm{T}}^{\gamma} > 130$ GeV and $|\eta^{\gamma}| < 2.5$. A large set of DM simplified model samples are generated, with mediator mass (M_{med}) ranging from 1–2000 GeV and dark matter mass (M_{DM}) ranging from 1–1000 GeV. In the same way, EW-DM effective interaction samples are generated at LO in a range of 1–1000 GeV for the DM particle mass. The ADD signal samples are generated at LO using PYTHIA 8.240, requiring $E_{\mathrm{T}}^{\gamma} > 130$ GeV, with no restriction on the photon η. Samples are generated in a grid of values for the $n = 3$–6 and $M_{\mathrm{D}} = 1$–6 TeV scenarios. The efficiency of the full event selection for these signal models ranges from 6 to 29% for the simplified DM models, from 44% to 46% for the EW-DM model, and from 23% to 30% for the ADD model, depending on the parameters of the models.

V. BACKGROUND ESTIMATION

The primary irreducible background for the $\gamma + p_{\mathrm{T}}^{\mathrm{miss}}$ signature is SM Z boson production in association with a photon, $Z(\to \nu\bar{\nu}) + \gamma$. Other SM background processes include $W(\to \ell\bar{\nu}) + \gamma$ (where the charged lepton ℓ is undetected), $W \to \ell\nu$ (where ℓ is falsely identified as a photon), $\gamma +$ jets, QCD multijet events (with a jet misidentified as a photon), $\gamma\gamma$, tγ, $t\bar{t}\gamma$, VVγ (where V refers to a W or a Z boson), and $Z(\to \ell\overline{\ell}) + \gamma$. In addition, a small residual number of events from noncollision sources, such as beam halo interactions [36], contribute to the total background. The background estimation and signal extraction are performed concurrently via a simultaneous maximum likelihood (ML) fit across the signal region and the corresponding single-lepton and dilepton CRs. A global likelihood function is constructed to model the expected background contributions in each bin of the E_{T}^{γ} variable in both SR and CRs, as well as the expected signal yield in each SR bin. The best-fit background model and signal strength are obtained by maximizing the likelihood function. The likelihood function is defined in the same way as described in Ref. [10]. Separate approaches are adopted to estimate the dominant $Z(\to \nu\bar{\nu}) + \gamma$ and $W(\to \ell\bar{\nu}) + \gamma$ backgrounds, and subdominant backgrounds, as detailed below.

A. The $Z(\to \nu\bar{\nu}) + \gamma$ and $W(\to \ell\bar{\nu}) + \gamma$ background

The estimated per-bin SR yields of the $Z(\to \nu\bar{\nu}) + \gamma$ and $W(\to \ell\bar{\nu}) + \gamma$ backgrounds are scaled by transfer factors from the observed yields in the dilepton and single lepton CRs, respectively. The transfer factors are computed from simulation. In addition, to account for correlations between Z and W boson production, we compute from simulation a ratio that normalizes the $W(\to \ell\bar{\nu}) + \gamma$ yield to the $Z(\to \nu\bar{\nu}) + \gamma$ yield. Thus, the free background parameters in the likelihood function are the $Z(\to \nu\bar{\nu}) + \gamma$ SR bin yields, which account for both $V + \gamma$ processes. This approach allows cancellation of theoretical uncertainties common to $W\gamma$ and $Z\gamma$ production, such as PDF and scale uncertainties.

The simultaneous likelihood fit used for signal extraction relies on accurate predictions of the ratios between the dominant backgrounds in the SR and CRs, as well as on the absolute normalization and shape of the E_{T}^{γ} distributions for the subdominant backgrounds. To achieve the most

accurate possible predictions for these quantities, multiple correction factors are applied to each MC simulated sample of $V+\gamma$ processes. The first correction uses the selection efficiency factor ρ [28], which compensates for minor variations between simulated and observed reconstruction and identification efficiencies across different particle candidates. This ρ factor typically deviates from unity by only a few percent. A second adjustment implements higher-order QCD corrections, aligning the generator-level E_{T}^{γ} distributions with NNLO QCD calculations from the DYRES program [37]. Finally, a third modification incorporates NLO-EW effects (as taken from Refs. [38,39]) on E_{T}^{γ} distributions, derived from these references and updated with the LUXqed17 PDF set [40].

B. Electron misidentification background

Another key background originates from $W \to e\nu$ events where an electron is mistakenly identified as a photon. Misidentification occurs when hits in the upstream tracker layers along the electron trajectory are missed. A seeding efficiency of ϵ for electrons with $p_{\mathrm{T}} > 160$ GeV is measured in data using a tag-and-probe [41] technique in $Z \to e+e-$ events, and is validated through MC simulation. Misidentified electron events are modeled using a proxy sample of electron events, selected from the data by requiring an ECAL cluster with a pixel seed. These proxy events must satisfy the same selection criteria as those used for the signal candidate events except for the substitution of an electron for a photon candidate. The number of electron proxy events is then scaled by $R_{\epsilon} = (1-\epsilon)/\epsilon$ to estimate the contribution from electron misidentification to our signal candidate selection. The ratio R_{ϵ} was measured to be 0.030 ± 0.003 and was found to be uniform across the considered E_{T}^{γ} spectrum. The dominant uncertainty in this estimate arises from the statistical uncertainty in the measurement of ϵ.

C. Jet misidentification background

EM showers originating from hadronic activity can be misidentified as a photon signature. To estimate this background, the number of events are compared in two different subsets of a low–$p_{\mathrm{T}}^{\mathrm{miss}}$ multijet data sample, where low–$p_{\mathrm{T}}^{\mathrm{miss}}$ is defined as $p_{\mathrm{T}}^{\mathrm{miss}} < 30$ GeV. The "first subset" includes events with a photon candidate that meets the signal selection criteria, containing both true photons and jets that are misidentified as photons. The "second subset" consists of events where the photon candidate satisfies less stringent shower shape requirements ($\sigma_{i\eta i\eta} > 0.0103$) and inverted isolation criteria compared to the signal candidates. The jet misidentification rate is then defined as the ratio of misidentified events in the first subset to the total number of events in the second subset.

The numerator is estimated by fitting the observed $\sigma_{i\eta i\eta}$ distribution of the photon candidate in the first subset using a combination of simulated distributions and those derived from the observed data. For genuine photons, the shower width distribution is created using simulated $\gamma+$jets events. For jets that are misidentified as photons, the distribution is obtained from a sample selected by inverting the charged-hadron isolation criteria and completely removing the shower shape requirement as both variables are correlated with each other.

The jet misidentification rate is measured to be between 0.01 to 0.16 across the E_{T}^{γ} spectrum, with relative uncertainties between 1.7 and 18.8%. The systematic uncertainties in this measurement are dominant, comprising the shower shape distribution fit and shower shape modeling uncertainty, variations in the charged-hadron isolation threshold, low–$p_{\mathrm{T}}^{\mathrm{miss}}$ requirement, and template bin width.

To estimate the background from jets misidentified as photons in the signal sample, the hadron misidentification rate is multiplied by the number of events in the high–$p_{\mathrm{T}}^{\mathrm{miss}}$ CR, defined as $p_{\mathrm{T}}^{\mathrm{miss}} > 200$ GeV. These events include a photon candidate that passes the same selection criteria as used for the second subset of the low–$p_{\mathrm{T}}^{\mathrm{miss}}$ CR.

D. Beam halo background

Beam halo background estimates are obtained by fitting the angular distributions of the calorimeter clusters. Energy clusters in the ECAL caused by beam halo muons are observed to concentrate around $|\sin(\phi)| \sim 0$, whereas photon candidates from all other collision-related processes are uniformly distributed around ϕ [36]. This motivates the split of the SR into two parts according to ϕ to constrain the beam halo normalization as mentioned in Sec. III.

The partition of the SR can be thought of as a two-bin fit. Collision processes occupy the relative fractions of phase space in the horizontal (H) and vertical (V) SR, $C_H = 1/\pi$ and $C_V = (\pi-1)/\pi$, respectively. For beam halo events, the corresponding fractions are determined by selecting a halo-enriched sample where the halo-veto identification criteria are inverted. Thus, a fit of the two subsets of the SR provides an estimate of the overall normalization of the beam halo background.

E. Other minor SM background processes

The SM $t\bar{t}\gamma$, VVγ, $Z(\to \ell\bar{\ell}) + \gamma$, and $\gamma+$jets processes together account for about 10% of the background processes in the SR. Although $Z(\to \ell\bar{\ell}) + \gamma$ and $\gamma+$jets do not involve high-p_{T} invisible particles, the former can exhibit large $p_{\mathrm{T}}^{\mathrm{miss}}$ when the leptons fail to be reconstructed, and the latter when jet energy is severely mismeasured. These backgrounds are estimated using MC simulation.

VI. SYSTEMATIC UNCERTAINTIES

The systematic uncertainty sources taken into account for the E_{T}^{γ} distribution ratios among the $V+\gamma$ processes are PDFs, higher-order QCD corrections, higher-order EW

TABLE III. Summary of systematic uncertainties considered in the analysis. "W/Z Ratio" refers to correlated uncertainties propagated from $W(\to \ell\bar{\nu}) + \gamma$ to $Z(\to \nu\bar{\nu}) + \gamma$ background estimation (due to higher-order corrections and PDFs), "TF" denotes transfer factors, "MisID" represents misidentification backgrounds (electrons or jets misidentified as photons), and "Other" includes additional minor backgrounds.

Systematic Uncertainty	W/Z Ratio	W TF	Z TF	Other Background	Electron MisID	Jet MisID	Halo
NNLO QCD, EW, PDF	Shape (1–10%)	···	···	···	···	···	···
Photon ID SF	···	···	···	Shape (3–11%)	···	···	···
MisID rate	···	···	···	···	Shape (5–8%)	Shape (1–10%)	···
Halo	···	···	···	···	···	···	Shape (2–30%)
Jet energy scale	···	···	···	Shape (4–20%)	···	···	···
Photon energy scale	···	···	···	Shape (5.5–20%)	···	···	···
Integrated luminosity	···	Flat (1–2%)	Flat (1–2%)	Flat (1–2%)	···	···	···
Lepton identification	Flat (1–2%)	Flat (1–2%)	Flat (1–2%)	···	···	···	···
MC and CR statistical	···	···	···	Bin-by-bin	···	···	···

corrections, and data-to-simulation efficiency correction factors ρ. The PDF uncertainty is determined by varying the weight of each event using the weights provided in the NNPDF set, and taking the variance among the resulting E_{T}^{γ} distributions. This uncertainty is treated as fully correlated across different bins of p_{T} in the ratio between the $Z(\to \nu\bar{\nu}) + \gamma$ and $W(\to \ell\bar{\nu}) + \gamma$ processes, i.e., the variation of the ratio is constrained by the ratios of the upward and downward variations. Uncertainties related to higher-order QCD corrections are considered uncorrelated in the ratio between the $Z(\to \nu\bar{\nu}) + \gamma$ and $W(\to \ell\bar{\nu}) + \gamma$ processes. Since EW corrections become more significant at higher E_{T}^{γ} but are only known to NLO accuracy, their uncertainties are estimated using a particular method described in Ref. [42], by assigning separate nuisance parameters to account for the uncertainty in the overall scale of the correction and its residual shape dependence with E_{T}^{γ}. Additionally, the full correction due to photon-induced $Z + \gamma$ and $W + \gamma$ production cross sections is considered as an uncertainty. Finally, the data-to-simulation correction factors ρ for lepton identification efficiencies come with associated uncertainties that do not cancel out when calculating ratios between regions defined by different lepton selection criteria. All four uncertainties are treated as correlated across the E_{T}^{γ} bins.

Other smaller experimental uncertainties that affect the final background estimates include the integrated luminosity, jet and γ energy scales, $p_{\mathrm{T}}^{\mathrm{miss}}$ resolution, and data-to-simulation scale factors for object identification. Table III presents an overview of the systematic uncertainties considered in this analysis. In this table, "shape" indicates uncertainties that impact the shape of the distributions. This means that the uncertainty can vary differently among bins in a histogram. Uncertainties affecting only the overall normalization ("flat") are modeled by nuisance parameters with a log-normal prior. A 3% to 11% uncertainty is applied to account for the photon identification efficiency differences between data and simulation. The electron misidentification rate uncertainty (5%–8%) and jet misidentification rate (1%–10%) uncertainty both impact the shape of the estimated background distribution. Beam halo effects contribute to the halo background uncertainty (2%–30%), which is treated as a shape uncertainty due to its nonuniform distribution in the detector. This uncertainty is obtained by varying the selection used to construct the beam-halo control sample. Shape uncertainties are also considered for the jet energy scale (4%–20%) and photon energy scale (5.5%–20%). Lepton identification scale factor uncertainties (muon 1%, electron 2%) are treated as flat across both W and Z transfer factors, impacting only the normalization of the estimated background. The integrated luminosity uncertainty is treated as a flat uncertainty, uniformly affecting all processes. It is estimated to be 1.2%–2.5%, partially correlated between the data-taking years [43–45]. Finally, MC and CR statistical uncertainties are treated bin-by-bin to account for statistical variations in the background estimation.

Among the listed uncertainties, theoretical uncertainties and those arising from photon and lepton identification efficiencies have the most significant impact on the signal extraction fit. In the combined likelihood for the different data-taking years, systematic uncertainties are classified as either correlated or uncorrelated. Correlated uncertainties include jet energy scale, photon energy scale, and integrated luminosity, while uncorrelated uncertainties include factors such as photon identification and electron and jet misidentification rates, as well as theoretical uncertainties in the transfer factors.

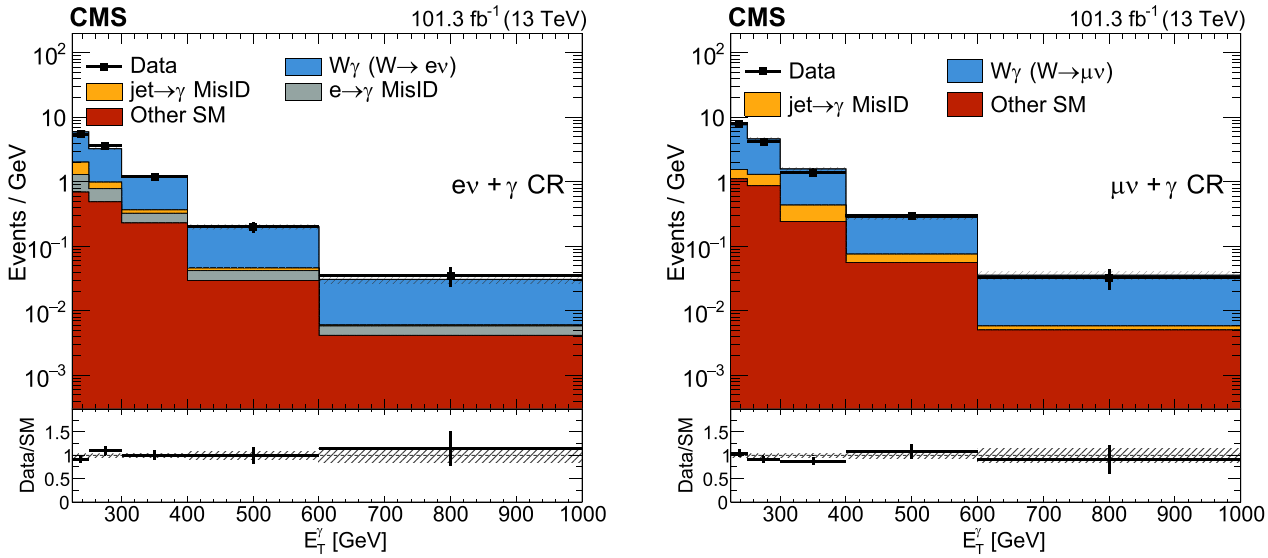

FIG. 4. Comparison of data and background postfit distributions in the $e\nu + \gamma$ (left) and $\mu\nu + \gamma$ (right) CRs for the combination of 2017 and 2018 datasets. The last bin of the distribution includes the overflow events. The ratios of data to the background predictions are shown in the lower panels, with the cross hatched uncertainty bands including the combination of all systematic uncertainties.

VII. RESULTS

A. Signal extraction

The potential signal contribution is extracted from the data by performing a simultaneous fit to the E_T^γ distributions in the SR and CRs. Uncertainties in several quantities are modeled as nuisance parameters in the fitting process.

The free parameter of the likelihood function is the signal strength modifier (μ), which, for a given signal hypothesis, controls the signal normalization relative to the model cross section.

B. Postfit distributions

The result is extracted using the maximum likelihood fit approach provided by the CMS statistical analysis tool COMBINE [46]. Figures 4 and 5 show the observed postfit distributions of E_T^γ in the four CRs, while Fig. 6 shows the expected E_T^γ distributions in the vertical and horizontal SR using the combined 2017 and 2018 dataset. Table IV shows the corresponding total yields, categorized by process, in the vertical and horizontal SR.

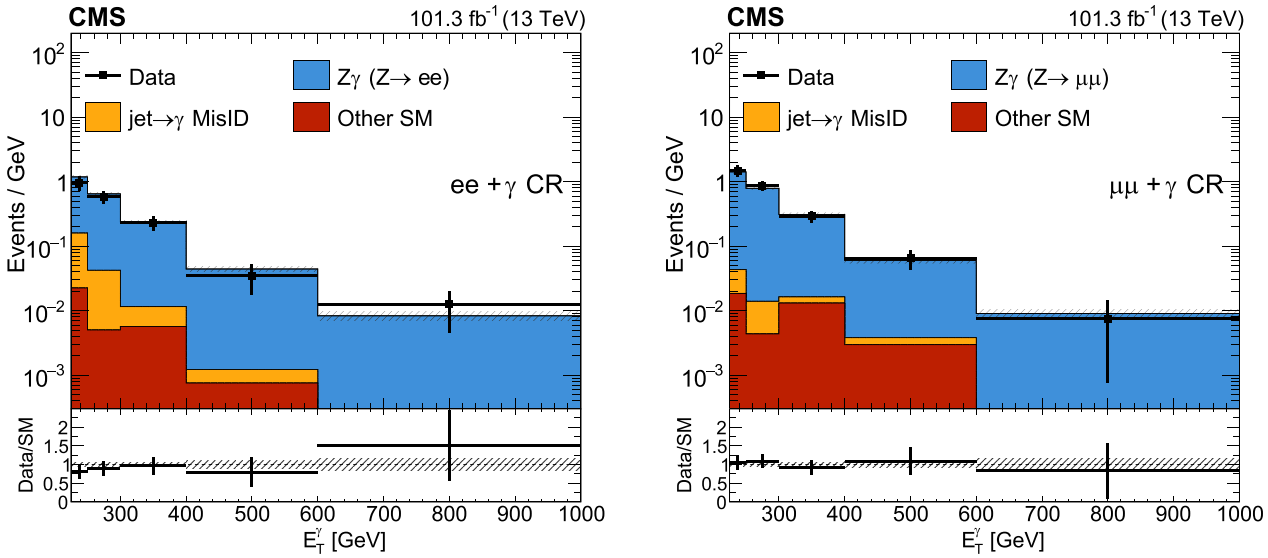

FIG. 5. Comparison of data and background postfit distributions in the $ee + \gamma$ (left) and $\mu\mu + \gamma$ (right) CRs for the combination of 2017 and 2018 datasets. The last bin of the distribution includes the overflow events. The ratios of data to the background predictions are shown in the lower panels, with the cross hatched uncertainty bands including the combination of all systematic uncertainties.

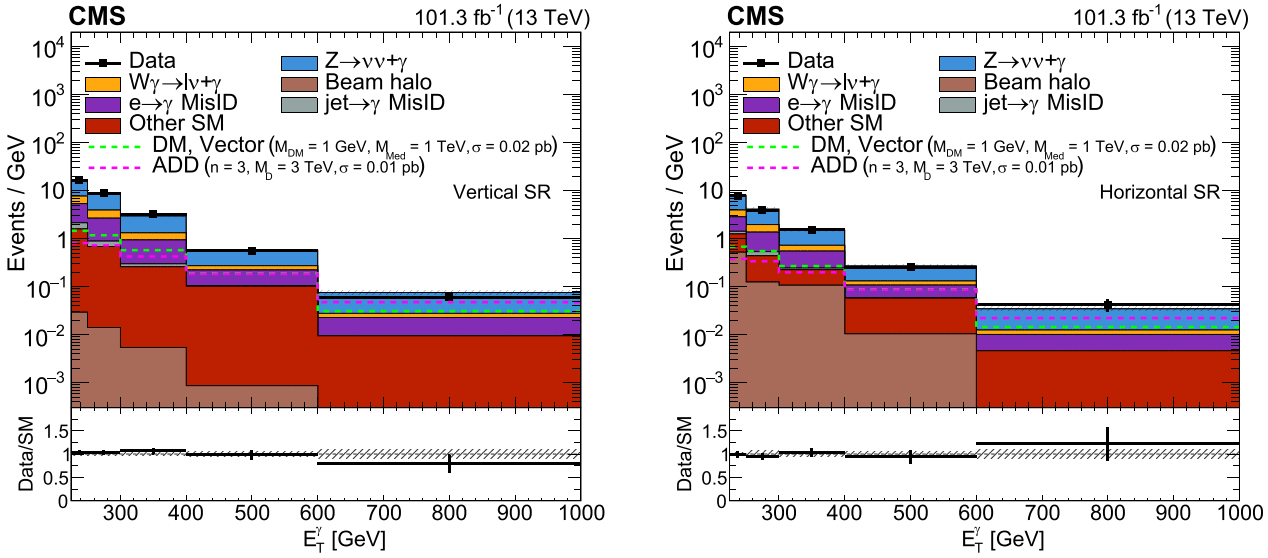

FIG. 6. Comparison of data and background postfit distributions for the vertical (left) and horizontal (right) regions for the combination of 2017 and 2018 datasets. Templates for signal hypotheses are shown overlaid as light green and magenta dashed lines along with their cross section values. The last bin of the distribution includes the overflow events.

The final result is obtained by performing a simultaneous fit that combines the previously published 2016 analysis [10] with the 2017 and 2018 datasets. These datasets are fitted using a common likelihood function, while the systematic uncertainties, including those carried over from the 2016 analysis, are detailed in Sec. VI.

C. Limits and constraints

No significant excess of events beyond the SM expectation is observed. Upper limits are determined for the production cross section of three new physics processes mentioned in Sec. I. For each model, a 95% confidence level (CL) upper limit is obtained utilizing the asymptotic CL_s criterion [47–49], with a test statistic based on the negative logarithm of the likelihood in Sec. VII A.

The simplified DM model parameters proposed by the ATLAS-CMS Dark Matter Forum Ref. [7] are intended to enable the comparison and translation of various DM search results. Figure 7 illustrates the 95% CL upper cross section limits relative to the corresponding theoretical cross section ($\mu_{95} = \sigma_{95\%}/\sigma_{\text{theory}}$) for the vector and axial-vector mediator scenarios in the M_{med}–M_{DM} plane. The solid red (black) curves represent the expected (observed) contour where $\mu_{95} = 1$. The dotted line above (or below) the expected contour indicates the $\pm 1\sigma$ uncertainty band on the expected limit. For the simplified DM NLO models considered, mediator masses up to 1085 GeV are excluded for M_{DM} values less than 50 GeV for both vector and axial vector mediator. The apparent difference between the good agreement observed in Fig. 6 and the observed limits shown in Fig. 7 arises because Fig. 6 presents the 2017–2018

TABLE IV. Total yield in vertical and horizontal regions using the combined 2017 and 2018 dataset.

	Prefit		Postfit	
Process	Vertical	Horizontal	Vertical	Horizontal
$Z(\to \nu\bar{\nu}) + \gamma$	621 ± 33	290 ± 16	688 ± 20	321 ± 9
$W(\to \ell\bar{\nu}) + \gamma$	174 ± 7	81 ± 3	172 ± 5	80 ± 3
Electron misidentification	257 ± 7	117 ± 3	262 ± 7	120 ± 3
QCD	28 ± 1.0	11 ± 0.2	28 ± 1	11 ± 0.2
Beam halo	1.85 ± 0	26 ± 21	2.2 ± 0.2	32 ± 18
$t\bar{t}\gamma/t\gamma$	28 ± 2	13 ± 1	28 ± 2	13 ± 1
Other background	96 ± 5	45 ± 2	94 ± 5	43 ± 2
Total background	1204 ± 35	583 ± 27	1275 ± 22	622 ± 21
ADD ($M_{\text{D}} = 3$, n = 3)	155	72	0	0
DM ($M_{\text{med}} = 1$, $M_{\text{DM}} = 1$)	203	95	0	0
Data	1315	613	1315	613

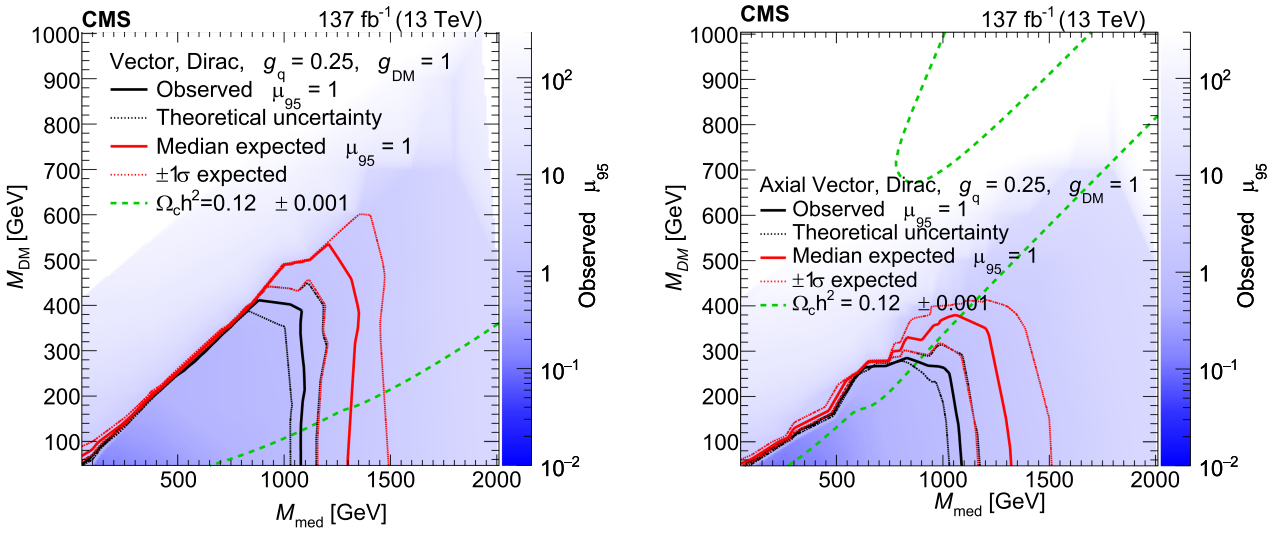

FIG. 7. The ratio of 95% CL upper cross section limits to the theoretical cross section (μ_{95}), for simplified DM models with vector (left) and axial-vector (right) mediators, using the full 2016–2018 dataset corresponding to an integrated luminosity of 137 fb^{-1}, assuming $g_q = 0.25$ and $g_{\mathrm{DM}} = 1$. Expected $\mu_{95} = 1$ contours are overlaid in red. The region below and to the left of the observed contour is excluded. For simplified DM model parameters in the region below the lower green dash contour, and also above the corresponding upper contour in the right hand plot, cosmological DM abundance exceeds the density observed by the Planck satellite experiment.

postfit SR distributions, whereas Fig. 7 is based on the combined 2016–2018 datasets. The combined observed limit reflects statistical fluctuations present in the 2016 data-taking period.

Results for vector and axial-vector mediators are then compared with constraints established by the cosmic microwave background measurements of the cosmological relic density of DM by the Planck satellite experiment [50]. For each model separately, the expected DM abundance is estimated using the thermal freeze-out mechanism implemented in the MADDM framework [51] and is then compared to the observed cold DM density, $\Omega_c h^2 = 0.12 \pm 0.001$ [50], where Ω_c represents the DM relic abundance and h is the dimensionless Hubble constant.

The exclusion contours in Fig. 7 are converted into the σ_{SI}, σ_{SD}–M_{DM} plane, where σ_{SI} and σ_{SD} represent the spin-independent and spin-dependent DM–nucleon scattering cross sections, respectively, as depicted in Fig. 8. The procedure for this translation and the presentation of results follows the prescription outlined in Ref. [8]. Specifically, to facilitate a direct comparison with direct-detection experiments, these limits are computed at 90% CL [7]. Compared to direct-detection experiments, this search sets more stringent limits for DM masses under 2 GeV in the spin-independent scenario and below 200 GeV in the spin-dependent case.

For the DM model characterized by a contact interaction of type $\gamma\gamma\chi\bar{\chi}$, upper limits are established on the production cross section, which are subsequently translated into lower limits on the suppression scale Λ for $k_1 = k_2 = 1.0$. The observed (expected) 95% CL lower limits on Λ as a function of the DM mass M_{DM} are shown in Fig. 9. For M_{DM} values ranging from 1 to 800 GeV, Λ values up to 940 GeV are excluded at 95% CL, with an expected exclusion up to 1000 GeV, using the dataset corresponding to an integrated luminosity of 137 fb^{-1}.

Figure 10 shows the upper limit and the theoretically calculated ADD graviton production cross section for $n = 3$ extra dimensions, as a function of M_{D}. The lower limit on M_{D} as a function of n extra dimensions is shown in Fig. 11. The limit is nearly constant across extra dimensions ($n = 3$ to $n = 6$), excluding M_{D} values up to 3.2 (3.7) TeV, observed (expected), with the current analysis, providing stronger constraints on large extra dimensions than previous searches.

These limits provide important constraints on simplified DM models, effective EW–DM contact interactions, and large extra dimension scenarios using the monophoton final state at the LHC.

VIII. SUMMARY

Proton-proton collisions producing a high transverse momentum photon and large missing transverse momentum have been investigated to search for new phenomena, using a dataset corresponding to 137 fb^{-1} of integrated luminosity recorded at $\sqrt{s} = 13$ TeV at the LHC. No deviations from the standard model predictions are observed. For the simplified dark matter production models considered, the observed (expected) lower limit on the

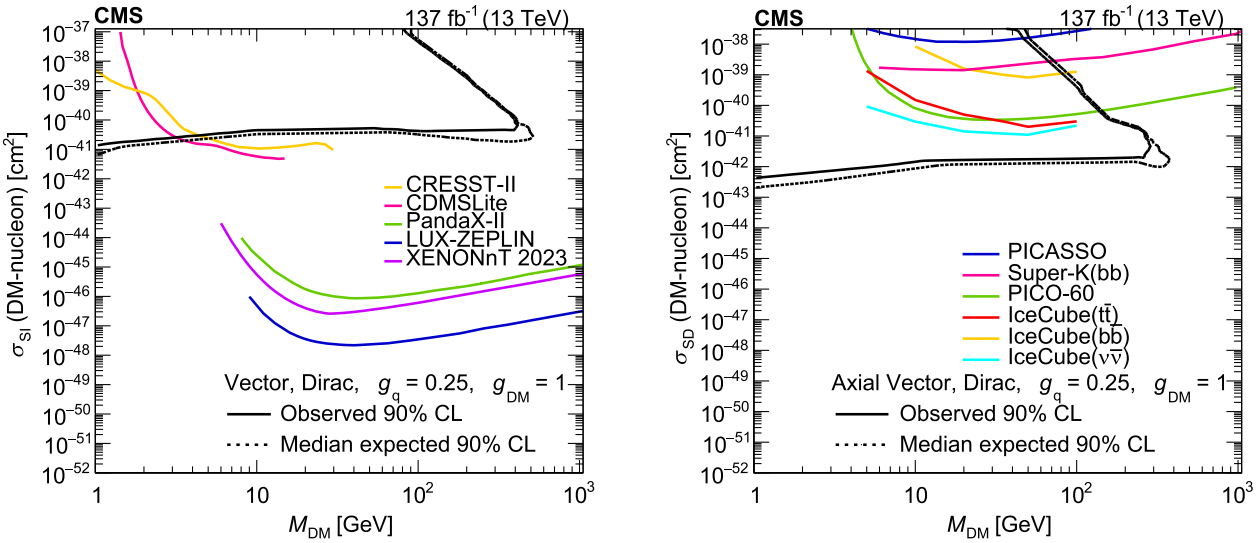

FIG. 8. The 90% CL exclusion limits on the χ–nucleon spin-independent (left) and spin-dependent (right) scattering cross sections involving vector and axial-vector operators, respectively, are shown as a function of M_{DM}, using the 2016–2018 dataset. Simplified model DM parameters $g_q = 0.25$ and $g_{\mathrm{DM}} = 1$ are assumed. Also shown are corresponding exclusion contours, where regions above the curves are excluded, from recent results by the CDMSLite [52], LUX-ZEPLIN [53], PandaX-II [54], XENONnT [55], CRESST-II [56], PICO-60 [57], IceCube [58], PICASSO [59], and Super-Kamiokande [60] Collaborations.

mediator mass is 1085 (1300) GeV in both cases for a 1 GeV dark matter particle mass. For an effective electroweak dark matter contact interaction, the observed (expected) lower limit on the suppression parameter Λ is 940 (1000) GeV, which is an improvement of 10% (5%) over the 2016 analysis, while for the model with extra spatial dimensions, values of the effective Planck scale M_{D} up to 3.2 TeV are excluded between 3 and 6 extra dimensions, improving upon the 2016 results by 10% (11%). These results set the most stringent limits to date on these parameters of the electroweak contact interaction and extra dimension models in the monophoton final state. The improvement in the expected limits obtained with the full 2016–2018 dataset on the parameters of the model is modest, of the order of 10%–14% (30%–40% in the expected cross sections limits) compared to 2016.

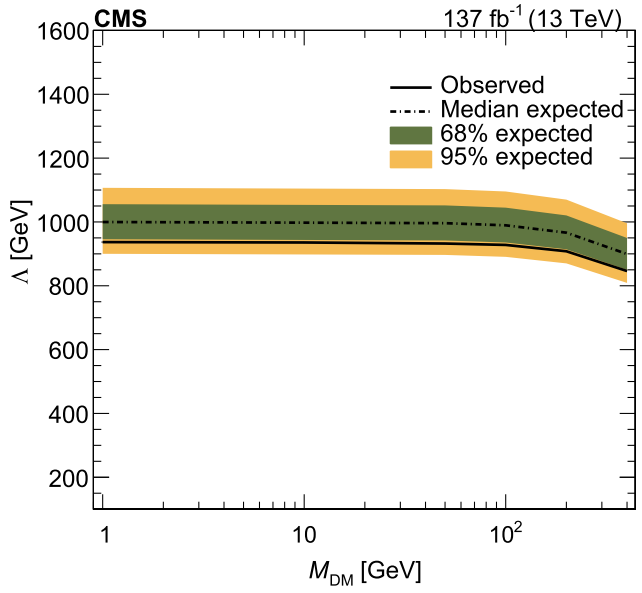

FIG. 9. The 95% CL observed and expected lower limits on Λ for an effective EW–DM contact interaction, as a function of M_{DM} using the 2016–2018 dataset corresponding to an integrated luminosity of 137 fb^{-1}.

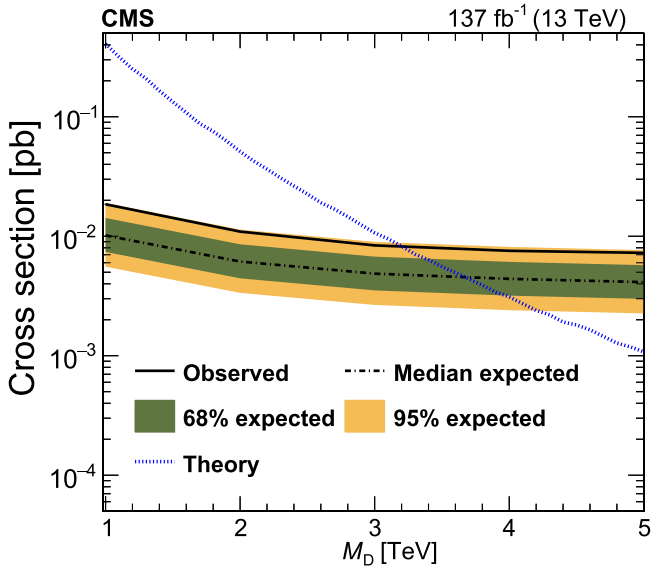

FIG. 10. The 95% CL upper limits on the ADD graviton production cross section as a function of M_{D}, for $n = 3$ extra dimensions.

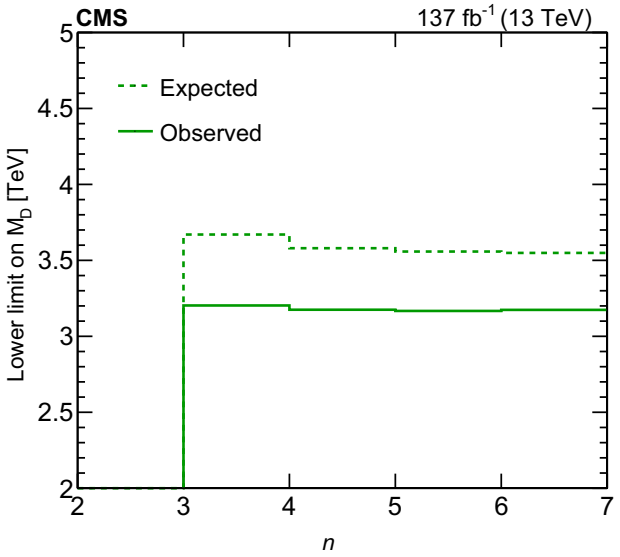

FIG. 11. Lower limit on the fundamental Planck scale M_D as a function of the number of extra dimensions n, using the 2016–2018 datasets with an integrated luminosity of 137 fb^{-1}.

This occurs for two reasons. First, the increased instantaneous luminosity of the collider in the later data-taking years necessitated higher thresholds on p_T^{miss} and E_T^γ in the trigger. The corresponding adjustments in the event selection result in a reduction of acceptance, and of the lever arm for distinguishing signal from background in the shape of the E_T^γ distributions. Second, because systematic uncertainties, mainly the theoretical QCD scale and electroweak uncertainties in the $Z(\to \nu\bar{\nu}) + \gamma$ and $W(\to \ell\bar{\nu}) + \gamma$ backgrounds, become more significant relative to the diminished statistical uncertainties of the full sample.

ACKNOWLEDGMENTS

We congratulate our colleagues in the CERN accelerator departments for the excellent performance of the LHC and thank the technical and administrative staffs at CERN and at other CMS institutes for their contributions to the success of the CMS effort. In addition, we gratefully acknowledge the computing centers and personnel of the Worldwide LHC Computing Grid and other centers for delivering so effectively the computing infrastructure essential to our analyses. Finally, we acknowledge the enduring support for the construction and operation of the LHC, the CMS detector, and the supporting computing infrastructure provided by the following funding agencies: SC (Armenia), BMBWF and FWF (Austria); FNRS and FWO (Belgium); CNPq, CAPES, FAPERJ, FAPERGS, and FAPESP (Brazil); MES and BNSF (Bulgaria); CERN; CAS, MoST, and NSFC (China); MINCIENCIAS (Colombia); MSES and CSF (Croatia); RIF (Cyprus); SENESCYT (Ecuador); ERC PRG, TARISTU24-TK10 and MoER TK202 (Estonia); Academy of Finland, MEC, and HIP (Finland); CEA and CNRS/IN2P3 (France); SRNSF (Georgia); BMFTR, DFG, and HGF (Germany); GSRI (Greece); NKFIH (Hungary); DAE and DST (India); IPM (Iran); SFI (Ireland); INFN (Italy); MSIT and NRF (Republic of Korea); MES (Latvia); LMTLT (Lithuania); MOE and UM (Malaysia); BUAP, CINVESTAV, CONACYT, LNS, SEP, and UASLP-FAI (Mexico); MOS (Montenegro); MBIE (New Zealand); PAEC (Pakistan); MES, NSC, and NAWA (Poland); FCT (Portugal); MESTD (Serbia); MICIU/AEI and PCTI (Spain); MOSTR (Sri Lanka); Swiss Funding Agencies (Switzerland); MST (Taipei); MHESI (Thailand); TUBITAK and TENMAK (Türkiye); NASU (Ukraine); STFC (United Kingdom); DOE and NSF (USA). Individuals have received support from the Marie-Curie program and the European Research Council and Horizon 2020 Grant, Contracts No. 675440, No. 724704, No. 752730, No. 758316, No. 765710, No. 824093, No. 101115353, No. 101002207, No. 101001205, and COST Action No. CA16108 (European Union); the Leventis Foundation; the Alfred P. Sloan Foundation; the Alexander von Humboldt Foundation; the Science Committee, project no. 22rl-037 (Armenia); the Fonds pour la Formation à la Recherche dans l'Industrie et dans l'Agriculture (FRIA) and Fonds voor Wetenschappelijk Onderzoek contract No. 1228724N (Belgium); the Beijing Municipal Science & Technology Commission, No. Z191100007219010, the Fundamental Research Funds for the Central Universities, the Ministry of Science and Technology of China under Grant No. 2023YFA1605804, the Natural Science Foundation of China under Grants No. 12061141002, No. 12535004, and USTC Research Funds of the Double First-Class Initiative No. YD2030002017 (China); the Ministry of Education, Youth and Sports (MEYS) of the Czech Republic; the Shota Rustaveli National Science Foundation, Grant No. FR-22-985 (Georgia); the Deutsche Forschungsgemeinschaft (DFG), among others, under Germany's Excellence Strategy—EXC 2121 "Quantum Universe"—390833306, and under project number 400140256-GRK2497; the Hellenic Foundation for Research and Innovation (HFRI), Project Number 2288 (Greece); the Hungarian Academy of Sciences, the New National Excellence Program—ÚNKP, the NKFIH research Grants No. K 131991, No. K 133046, No. K 138136, No. K 143460, No. K 143477, No. K 146913, No. K 146914, No. K 147048, No. 2020-2.2.1-ED-2021-00181, No. TKP2021-NKTA-64, and No. 2021-4.1.2-NEMZ_KI-2024-00036 (Hungary); the Council of Science and Industrial Research, India; ICSC—National Research Center for High Performance Computing, Big Data and Quantum Computing, FAIR—Future Artificial Intelligence Research, and CUP I53D23001070006 (Mission 4 Component 1), funded by the NextGenerationEU program (Italy); the Latvian Council

of Science; the Ministry of Education and Science, project no. 2022/WK/14, and the National Science Center, contracts Opus 2021/41/B/ST2/01369, 2021/43/B/ST2/01552, 2023/49/B/ST2/03273, and the NAWA contract BPN/PPO/2021/1/00011 (Poland); the Fundação para a Ciência e a Tecnologia, grant CEECIND/01334/2018 (Portugal); the National Priorities Research Program by Qatar National Research Fund; MICIU/AEI/10.13039/501100011033, ERDF/EU, "European Union NextGenerationEU/PRTR," and Programa Severo Ochoa del Principado de Asturias (Spain); the Chulalongkorn Academic into Its 2nd Century Project Advancement Project, the National Science, Research and Innovation Fund program IND_FF_68_369_2300_097, and the Program Management Unit for Human Resources & Institutional Development, Research and Innovation, Grant No. B39G680009 (Thailand); the Kavli Foundation; the Nvidia Corporation; the SuperMicro Corporation; the Welch Foundation, contract No. C-1845; and the Weston Havens Foundation (USA).

DATA AVAILABILITY

Release and preservation of data used by the CMS Collaboration as the basis for publications is guided by the CMS data preservation, re-use and open access policy [61].

[1] N. Arkani-Hamed, S. Dimopoulos, and G. Dvali, The hierarchy problem and new dimensions at a millimeter, Phys. Lett. B **429**, 263 (1998).
[2] N. Arkani-Hamed, S. Dimopoulos, and G. Dvali, Phenomenology, astrophysics, and cosmology of theories with submillimeter dimensions and TeV scale quantum gravity, Phys. Rev. D **59**, 086004 (1999).
[3] N. Arkani-Hamed, S. Dimopoulos, G. R. Dvali, and N. Kaloper, Infinitely large new dimensions, Phys. Rev. Lett. **84**, 586 (2000).
[4] M. Beltran, D. Hooper, E. W. Kolb, Z. A. C. Krusberg, and T. M. P. Tait, Maverick dark matter at colliders, J. High Energy Phys. 09 (2010) 037.
[5] J. Goodman, M. Ibe, A. Rajaraman, W. Shepherd, T. M. P. Tait, and H.-B. Yu, Constraints on dark matter from colliders, Phys. Rev. D **82**, 116010 (2010).
[6] P. J. Fox, R. Harnik, J. Kopp, and Y. Tsai, Missing energy signatures of dark matter at the LHC, Phys. Rev. D **85**, 056011 (2012).
[7] D. Abercrombie, Dark matter benchmark models for early LHC run-2 searches: Report of the ATLAS/CMS dark matter forum, Phys. Dark Universe **27**, 100371 (2020).
[8] A. Boveia *et al.*, Recommendations on presenting LHC searches for missing transverse energy signals using simplified *s*-channel models of dark matter, Phys. Dark Universe **27**, 100365 (2020).
[9] A. Nelson, L. M. Carpenter, R. Cotta, A. Johnstone, and D. Whiteson, Confronting the Fermi line with LHC data: An effective theory of dark matter interaction with photons, Phys. Rev. D **89**, 056011 (2014).
[10] CMS Collaboration, Search for new physics in final states with a single photon and missing transverse momentum in proton-proton collisions at $\sqrt{s} = 13$ TeV, J. High Energy Phys. 02 (2019) 074.
[11] ATLAS Collaboration, Search for dark matter in association with an energetic photon in pp collisions at $\sqrt{s} = 13$ TeV with the ATLAS detector, J. High Energy Phys. 02 (2021) 226.
[12] HEPData record for this analysis (2025), 10.17182/hepdata.166403.
[13] CMS Collaboration, The CMS experiment at the CERN LHC, J. Instrum. **3**, S08004 (2008).
[14] CMS Collaboration, Development of the CMS detector for the CERN LHC Run 3, J. Instrum. **19**, P05064 (2024).
[15] CMS Collaboration, Electron and photon reconstruction and identification with the CMS experiment at the CERN LHC, J. Instrum. **16**, P05014 (2021).
[16] CMS Collaboration, Performance of the CMS muon detector and muon reconstruction with proton-proton collisions at $\sqrt{s} = 13$ TeV, J. Instrum. **13**, P06015 (2018).
[17] CMS Collaboration, Description and performance of track and primary-vertex reconstruction with the CMS tracker, J. Instrum. **9**, P10009 (2014).
[18] CMS Collaboration, Performance of the CMS level-1 trigger in proton-proton collisions at $\sqrt{s} = 13$ TeV, J. Instrum. **15**, P10017 (2020).
[19] CMS Collaboration, The CMS trigger system, J. Instrum. **12**, P01020 (2017).
[20] CMS Collaboration, Performance of the CMS high-level trigger during LHC run 2, J. Instrum. **19**, P11021 (2024).
[21] CMS Collaboration, Technical proposal for the Phase-II upgrade of the CMS detector, Tech. Rep. No. CMS-TDR-15-02, CERN, 2015, 10.17181/CERN.VU8I.D59J.
[22] CMS Collaboration, Particle-flow reconstruction and global event description with the CMS detector, J. Instrum. **12**, P10003 (2017).
[23] M. Cacciari, G. P. Salam, and G. Soyez, The anti-k_T jet clustering algorithm, J. High Energy Phys. 04 (2008) 063.
[24] M. Cacciari, G. P. Salam, and G. Soyez, Fastjet user manual, Eur. Phys. J. C **72**, 1896 (2012).
[25] CMS Collaboration, Jet energy scale and resolution in the CMS experiment in pp collisions at 8 TeV, J. Instrum. **12**, P02014 (2017).
[26] CMS Collaboration, Performance of missing transverse momentum reconstruction in proton-proton collisions at $\sqrt{s} = 13$ TeV using the CMS detector, J. Instrum. **14**, P07004 (2019).
[27] CMS Collaboration, Jet algorithms performance in 13 TeV data, CMS Physics Analysis Summary, Report No. CMS-PAS-JME-16-003, CERN, 2017, https://cds.cern.ch/record/2256875.

[28] CMS Collaboration, Performance of photon reconstruction and identification with the CMS detector in proton-proton collisions at $\sqrt{s} = 8$ TeV, J. Instrum. **10**, P08010 (2015).
[29] CMS Collaboration, Performance of the reconstruction and identification of high-momentum muons in proton-proton collisions at $\sqrt{s} = 13$ TeV, J. Instrum. **15**, P02027 (2020).
[30] R. D. Ball *et al.* (NNPDF Collaboration), Parton distributions from high-precision collider data, Eur. Phys. J. C **77**, 663 (2017).
[31] J. Alwall, R. Frederix, S. Frixione, V. Hirschi, F. Maltoni, O. Mattelaer, H. S. Shao, T. Stelzer, P. Torrielli, and M. Zaro, The automated computation of tree-level and next-to-leading order differential cross sections, and their matching to parton shower simulations, J. High Energy Phys. 07 (2014) 079.
[32] T. Sjöstrand, S. Ask, J. R. Christiansen, R. Corke, N. Desai, P. Ilten, S. Mrenna, S. Prestel, C. O. Rasmussen, and P. Z. Skands, An introduction to PYTHIA 8.2, Comput. Phys. Commun. **191**, 159 (2015).
[33] CMS Collaboration, Event generator tunes obtained from underlying event and multiparton scattering measurements, Eur. Phys. J. C **76**, 155 (2016).
[34] S. Agostinelli (GEANT4 Collaboration), GEANT4—a simulation toolkit, Nucl. Instrum. Methods Phys. Res., Sect. A **506**, 250 (2003).
[35] J. Allison, GEANT4 developments and applications, IEEE Trans. Nucl. Sci. **53**, 270 (2006).
[36] S. Orfanelli, A. E. Dabrowski, M. Giunta, R. Loos, M. J. Ambrose, J. Mans, R. Rusack, K. Stifter, D. Stickland, F. Fabbri *et al.*, A novel beam halo monitor for the CMS experiment at the LHC, J. Instrum. **10**, P11011 (2015).
[37] S. Catani, D. de Florian, G. Ferrera, and M. Grazzini, Vector boson production at hadron colliders: transverse-momentum resummation and leptonic decay, J. High Energy Phys. 12 (2015) 047.
[38] A. Denner, S. Dittmaier, M. Hecht, and C. Pasold, NLO QCD and electroweak corrections to $W + \gamma$ production with leptonic W-boson decays, J. High Energy Phys. 04 (2015) 018.
[39] A. Denner, S. Dittmaier, M. Hecht, and C. Pasold, NLO QCD and electroweak corrections to $Z + \gamma$ production with leptonic Z-boson decays, J. High Energy Phys. 02 (2016) 057.
[40] A. V. Manohar, P. Nason, G. P. Salam, and G. Zanderighi, The photon content of the proton, J. High Energy Phys. 12 (2017) 046.
[41] CMS Collaboration, Measurement of the inclusive W and Z production cross sections in pp collisions at $\sqrt{s} = 7$ TeV with the CMS experiment, J. High Energy Phys. 10 (2011) 132.
[42] J. M. Lindert *et al.*, Precise predictions for V + jets dark matter backgrounds, Eur. Phys. J. C **77**, 829 (2017).
[43] CMS Collaboration, Precision luminosity measurement in proton-proton collisions at $\sqrt{s} = 13$ TeV in 2015 and 2016 at CMS, Eur. Phys. J. C **81**, 800 (2021).
[44] CMS Collaboration, CMS luminosity measurement for the 2017 data-taking period at $\sqrt{s} = 13$ TeV, CMS Physics Analysis Summary, Report No. CMS-PAS-LUM-17-004, CERN, 2018, https://cds.cern.ch/record/2621960.
[45] CMS Collaboration, CMS luminosity measurement for the 2018 data-taking period at $\sqrt{s} = 13$ TeV, CMS Physics Analysis Summary, Report No. CMS-PAS-LUM-18-002, CERN, 2019, https://cds.cern.ch/record/2676164.
[46] CMS Collaboration, The CMS statistical analysis and combination tool: Combine, Comput. Software Big Sci. **8**, 19 (2024).
[47] T. Junk, Confidence level computation for combining searches with small statistics, Nucl. Instrum. Methods Phys. Res., Sect. A **434**, 435 (1999).
[48] A. L. Read, Presentation of search results: The cl_s technique, J. Phys. G **28**, 2693 (2002).
[49] G. Cowan, K. Cranmer, E. Gross, and O. Vitells, Asymptotic formulae for likelihood-based tests of new physics, Eur. Phys. J. C **71**, 1554 (2011); **73**, 2501(E) (2013).
[50] P. A. R. Ade *et al.* (Planck Collaboration), Planck 2015 results. XIII. Cosmological parameters, Astron. Astrophys. **594**, A13 (2016).
[51] M. Backovic, K. Kong, and M. McCaskey, MadDM v.1.0: Computation of dark matter relic abundance using MadGraph5, Phys. Dark Universe **5–6**, 18 (2014).
[52] R. Agnese *et al.* (SuperCDMS Collaboration), New results from the search for low-mass weakly interacting massive particles with the CDMS low ionization threshold experiment, Phys. Rev. Lett. **116**, 071301 (2016).
[53] J. Aalbers *et al.* (LZ Collaboration), Dark matter search results from 4.2 tonne-years of exposure of the LUX-ZEPLIN (LZ) experiment, Phys. Rev. Lett. **135**, 011802 (2025).
[54] X. Cui *et al.* (PandaX-II Collaboration), Dark matter results from 54-ton-day exposure of the PandaX-II experiment, Phys. Rev. Lett. **119**, 181302 (2017).
[55] E. Aprile *et al.* (XENON Collaboration), First dark matter search with nuclear recoils from the XENONnT experiment, Phys. Rev. Lett. **131**, 041003 (2023).
[56] G. Angloher *et al.* (CRESST Collaboration), Results on light dark matter particles with a low-threshold CRESST-II detector, Eur. Phys. J. C **76**, 25 (2016).
[57] C. Amole *et al.* (PICO Collaboration), Dark matter search results from the PICO-60 C_3F_8 bubble chamber, Phys. Rev. Lett. **118**, 251301 (2017).
[58] R. Abbasi *et al.* (IceCube Collaboration), Search for GeV-scale dark matter annihilation in the Sun with IceCube DeepCore, Phys. Rev. D **105**, 062004 (2022).
[59] E. Behnke *et al.*, Final results of the PICASSO dark matter search experiment, Astropart. Phys. **90**, 85 (2017).
[60] K. Choi *et al.* (Super-Kamiokande Collaboration), Search for neutrinos from annihilation of captured low-mass dark matter particles in the Sun by Super-Kamiokande, Phys. Rev. Lett. **114**, 141301 (2015).
[61] CMS data availability statement, 10.7483/OPENDATA.CMS.1BNU.8V1W.

A. Hayrapetyan,[1] V. Makarenko,[1] A. Tumasyan,[1,b] W. Adam,[2] J. W. Andrejkovic,[2] L. Benato,[2] T. Bergauer,[2] M. Dragicevic,[2] C. Giordano,[2] P. S. Hussain,[2] M. Jeitler,[2,c] N. Krammer,[2] A. Li,[2] D. Liko,[2] M. Matthewman,[2] I. Mikulec,[2] J. Schieck,[2,c] R. Schöfbeck,[2,c] D. Schwarz,[2] M. Shooshtari,[2] M. Sonawane,[2] W. Waltenberger,[2] C.-E. Wulz,[2,c] T. Janssen,[3] H. Kwon,[3] D. Ocampo Henao,[3] T. Van Laer,[3] P. Van Mechelen,[3] J. Bierkens,[4] N. Breugelmans,[4] J. D'Hondt,[4] S. Dansana,[4] A. De Moor,[4] M. Delcourt,[4] F. Heyen,[4] Y. Hong,[4] P. Kashko,[4] S. Lowette,[4] I. Makarenko,[4] D. Müller,[4] J. Song,[4] S. Tavernier,[4] M. Tytgat,[4,d] G. P. Van Onsem,[4] S. Van Putte,[4] D. Vannerom,[4] B. Bilin,[5] B. Clerbaux,[5] A. K. Das,[5] I. De Bruyn,[5] G. De Lentdecker,[5] H. Evard,[5] L. Favart,[5] P. Gianneios,[5] A. Khalilzadeh,[5] F. A. Khan,[5] A. Malara,[5] M. A. Shahzad,[5] L. Thomas,[5] M. Vanden Bemden,[5] C. Vander Velde,[5] P. Vanlaer,[5] F. Zhang,[5] M. De Coen,[6] D. Dobur,[6] G. Gokbulut,[6] J. Knolle,[6] L. Lambrecht,[6] D. Marckx,[6] K. Skovpen,[6] N. Van Den Bossche,[6] J. van der Linden,[6] J. Vandenbroeck,[6] L. Wezenbeek,[6] S. Bein,[7] A. Benecke,[7] A. Bethani,[7] G. Bruno,[7] A. Cappati,[7] J. De Favereau De Jeneret,[7] C. Delaere,[7] A. Giammanco,[7] A. O. Guzel,[7] V. Lemaitre,[7] J. Lidrych,[7] P. Malek,[7] P. Mastrapasqua,[7] S. Turkcapar,[7] G. A. Alves,[8] M. Barroso Ferreira Filho,[8] E. Coelho,[8] C. Hensel,[8] T. Menezes De Oliveira,[8] C. Mora Herrera,[8,e] P. Rebello Teles,[8] M. Soeiro,[8] E. J. Tonelli Manganote,[8,f] A. Vilela Pereira,[8,e] W. L. Aldá Júnior,[9] H. Brandao Malbouisson,[9] W. Carvalho,[9] J. Chinellato,[9,g] M. Costa Reis,[9] E. M. Da Costa,[9] G. G. Da Silveira,[9,h] D. De Jesus Damiao,[9] S. Fonseca De Souza,[9] R. Gomes De Souza,[9] S. S. Jesus,[9] T. Laux Kuhn,[9,h] M. Macedo,[9] K. Mota Amarilo,[9] L. Mundim,[9] H. Nogima,[9] J. P. Pinheiro,[9] A. Santoro,[9] A. Sznajder,[9] M. Thiel,[9] F. Torres Da Silva De Araujo,[9,i] C. A. Bernardes,[10,h] T. R. Fernandez Perez Tomei,[10] E. M. Gregores,[10] B. Lopes Da Costa,[10] I. Maietto Silverio,[10] P. G. Mercadante,[10] S. F. Novaes,[10] B. Orzari,[10] Sandra S. Padula,[10] V. Scheurer,[10] A. Aleksandrov,[11] G. Antchev,[11] P. Danev,[11] R. Hadjiiska,[11] P. Iaydjiev,[11] M. Misheva,[11] M. Shopova,[11] G. Sultanov,[11] A. Dimitrov,[12] L. Litov,[12] B. Pavlov,[12] P. Petkov,[12] A. Petrov,[12] S. Keshri,[13] D. Laroze,[13] S. Thakur,[13] W. Brooks,[14] T. Cheng,[15] T. Javaid,[15] L. Wang,[15] L. Yuan,[15] Z. Hu,[16] Z. Liang,[16] J. Liu,[16] X. Wang,[16] G. M. Chen,[17,j] H. S. Chen,[17,j] M. Chen,[17,j] Y. Chen,[17] Q. Hou,[17] X. Hou,[17] F. Iemmi,[17] C. H. Jiang,[17] A. Kapoor,[17,k] H. Liao,[17] G. Liu,[17] Z.-A. Liu,[17,l] J. N. Song,[17,l] S. Song,[17] J. Tao,[17] C. Wang,[17,j] J. Wang,[17] H. Zhang,[17] J. Zhao,[17] A. Agapitos,[18] Y. Ban,[18] A. Carvalho Antunes De Oliveira,[18] S. Deng,[18] B. Guo,[18] Q. Guo,[18] C. Jiang,[18] A. Levin,[18] C. Li,[18] Q. Li,[18] Y. Mao,[18] S. Qian,[18] S. J. Qian,[18] X. Qin,[18] X. Sun,[18] D. Wang,[18] J. Wang,[18] H. Yang,[18] M. Zhang,[18] Y. Zhao,[18] C. Zhou,[18] S. Yang,[19] Z. You,[20] K. Jaffel,[21] N. Lu,[21] G. Bauer,[22,m,n] B. Li,[22,o] H. Wang,[22] K. Yi,[22,p] J. Zhang,[22] Y. Li,[23] Z. Lin,[24] C. Lu,[24] M. Xiao,[24,q] C. Avila,[25] D. A. Barbosa Trujillo,[25] A. Cabrera,[25] C. Florez,[25] J. Fraga,[25] J. A. Reyes Vega,[25] C. Rendón,[26] M. Rodriguez,[26] A. A. Ruales Barbosa,[26] J. D. Ruiz Alvarez,[26] N. Godinovic,[27] D. Lelas,[27] A. Sculac,[27] M. Kovac,[28] A. Petkovic,[28] T. Sculac,[28] P. Bargassa,[29] V. Brigljevic,[29] B. K. Chitroda,[29] D. Ferencek,[29] K. Jakovcic,[29] A. Starodumov,[29] T. Susa,[29] A. Attikis,[30] K. Christoforou,[30] A. Hadjiagapiou,[30] C. Leonidou,[30] C. Nicolaou,[30] L. Paizanos,[30] F. Ptochos,[30] P. A. Razis,[30] H. Rykaczewski,[30] H. Saka,[30] A. Stepennov,[30] M. Finger,[31,a] M. Finger Jr.,[31] E. Ayala,[32] E. Carrera Jarrin,[33] A. A. Abdelalim,[34,r,s] R. Aly,[34,t,r] M. Abdullah Al-Mashad,[35] A. Hussein,[35] H. Mohammed,[35] K. Ehataht,[36] M. Kadastik,[36] T. Lange,[36] C. Nielsen,[36] J. Pata,[36] M. Raidal,[36] N. Seeba,[36] L. Tani,[36] A. Milieva,[37] K. Osterberg,[37] M. Voutilainen,[37] N. Bin Norjoharuddeen,[38] E. Brücken,[38] F. Garcia,[38] P. Inkaew,[38] K. T. S. Kallonen,[38] R. Kumar Verma,[38] T. Lampén,[38] K. Lassila-Perini,[38] B. Lehtela,[38] S. Lehti,[38] T. Lindén,[38] N. R. Mancilla Xinto,[38] M. Myllymäki,[38] M. m. Rantanen,[38] S. Saariokari,[38] N. T. Toikka,[38] J. Tuominiemi,[38] H. Kirschenmann,[39] P. Luukka,[39] H. Petrow,[39] M. Besancon,[40] F. Couderc,[40] M. Dejardin,[40] D. Denegri,[40] P. Devouge,[40] J. L. Faure,[40] F. Ferri,[40] P. Gaigne,[40] S. Ganjour,[40] P. Gras,[40] G. Hamel de Monchenault,[40] M. Kumar,[40] V. Lohezic,[40] J. Malcles,[40] F. Orlandi,[40] L. Portales,[40] S. Ronchi,[40] M. Ö. Sahin,[40] A. Savoy-Navarro,[40,u] P. Simkina,[40] M. Titov,[40] M. Tornago,[40] F. Beaudette,[41] G. Boldrini,[41] P. Busson,[41] C. Charlot,[41] M. Chiusi,[41] T. D. Cuisset,[41] F. Damas,[41] O. Davignon,[41] A. De Wit,[41] T. Debnath,[41] I. T. Ehle,[41] B. A. Fontana Santos Alves,[41] S. Ghosh,[41] A. Gilbert,[41] R. Granier de Cassagnac,[41] L. Kalipoliti,[41] M. Manoni,[41] M. Nguyen,[41] S. Obraztsov,[41] C. Ochando,[41] R. Salerno,[41] J. B. Sauvan,[41] Y. Sirois,[41] G. Sokmen,[41] L. Urda Gómez,[41] A. Zabi,[41] A. Zghiche,[41] J.-L. Agram,[42,v] J. Andrea,[42] D. Bloch,[42] J.-M. Brom,[42] E. C. Chabert,[42] C. Collard,[42] G. Coulon,[42] S. Falke,[42] U. Goerlach,[42] R. Haeberle,[42] A.-C. Le Bihan,[42] M. Meena,[42] O. Poncet,[42] G. Saha,[42] P. Vaucelle,[42] A. Di Florio,[43] D. Amram,[44]

S. Beauceron,[44] B. Blancon,[44] G. Boudoul,[44] N. Chanon,[44] D. Contardo,[44] P. Depasse,[44] C. Dozen,[44,w] H. El Mamouni,[44] J. Fay,[44] S. Gascon,[44] M. Gouzevitch,[44] C. Greenberg,[44] G. Grenier,[44] B. Ille,[44] E. Jourd'huy,[44] I. B. Laktineh,[44] M. Lethuillier,[44] B. Massoteau,[44] L. Mirabito,[44] A. Purohit,[44] M. Vander Donckt,[44] J. Xiao,[44] D. Chokheli,[45] I. Lomidze,[45] Z. Tsamalaidze,[45,x] V. Botta,[46] S. Consuegra Rodríguez,[46] L. Feld,[46] K. Klein,[46] M. Lipinski,[46] D. Meuser,[46] P. Nattland,[46] V. Oppenländer,[46] A. Pauls,[46] D. Pérez Adán,[46] N. Röwert,[46] M. Teroerde,[46] C. Daumann,[47] S. Diekmann,[47] A. Dodonova,[47] N. Eich,[47] D. Eliseev,[47] F. Engelke,[47] J. Erdmann,[47] M. Erdmann,[47] B. Fischer,[47] T. Hebbeker,[47] K. Hoepfner,[47] F. Ivone,[47] A. Jung,[47] N. Kumar,[47] M. y. Lee,[47] F. Mausolf,[47] M. Merschmeyer,[47] A. Meyer,[47] F. Nowotny,[47] A. Pozdnyakov,[47] W. Redjeb,[47] H. Reithler,[47] U. Sarkar,[47] V. Sarkisovi,[47] A. Schmidt,[47] C. Seth,[47] A. Sharma,[47] J. L. Spah,[47] V. Vaulin,[47] S. Zaleski,[47] M. R. Beckers,[48] C. Dziwok,[48] G. Flügge,[48] N. Hoeflich,[48] T. Kress,[48] A. Nowack,[48] O. Pooth,[48] A. Stahl,[48] A. Zotz,[48] H. Aarup Petersen,[49] A. Abel,[49] M. Aldaya Martin,[49] J. Alimena,[49] S. Amoroso,[49] Y. An,[49] I. Andreev,[49] J. Bach,[49] S. Baxter,[49] M. Bayatmakou,[49] H. Becerril Gonzalez,[49] O. Behnke,[49] A. Belvedere,[49] F. Blekman,[49,y] K. Borras,[49,z] A. Campbell,[49] S. Chatterjee,[49] L. X. Coll Saravia,[49] G. Eckerlin,[49] D. Eckstein,[49] E. Gallo,[49,y] A. Geiser,[49] V. Guglielmi,[49] M. Guthoff,[49] A. Hinzmann,[49] L. Jeppe,[49] M. Kasemann,[49] C. Kleinwort,[49] R. Kogler,[49] M. Komm,[49] D. Krücker,[49] W. Lange,[49] D. Leyva Pernia,[49] K.-Y. Lin,[49] K. Lipka,[49,aa] W. Lohmann,[49,bb] J. Malvaso,[49] R. Mankel,[49] I.-A. Melzer-Pellmann,[49] M. Mendizabal Morentin,[49] A. B. Meyer,[49] G. Milella,[49] K. Moral Figueroa,[49] A. Mussgiller,[49] L. P. Nair,[49] J. Niedziela,[49] A. Nürnberg,[49] J. Park,[49] E. Ranken,[49] A. Raspereza,[49] D. Rastorguev,[49] L. Rygaard,[49] M. Scham,[49,cc,z] S. Schnake,[49,z] P. Schütze,[49] C. Schwanenberger,[49,y] D. Selivanova,[49] K. Sharko,[49] M. Shchedrolosiev,[49] D. Stafford,[49] M. Torkian,[49] F. Vazzoler,[49] A. Ventura Barroso,[49] R. Walsh,[49] D. Wang,[49] Q. Wang,[49] K. Wichmann,[49] L. Wiens,[49,z] C. Wissing,[49] Y. Yang,[49] S. Zakharov,[49] A. Zimermmane Castro Santos,[49] A. Albrecht,[50] A. R. Alves Andrade,[50] M. Antonello,[50] S. Bollweg,[50] M. Bonanomi,[50] K. El Morabit,[50] Y. Fischer,[50] M. Frahm,[50] E. Garutti,[50] A. Grohsjean,[50] A. A. Guvenli,[50] J. Haller,[50] D. Hundhausen,[50] G. Kasieczka,[50] P. Keicher,[50] R. Klanner,[50] W. Korcari,[50] T. Kramer,[50] C. c. Kuo,[50] F. Labe,[50] J. Lange,[50] A. Lobanov,[50] L. Moureaux,[50] M. Mrowietz,[50] A. Nigamova,[50] K. Nikolopoulos,[50] Y. Nissan,[50] A. Paasch,[50] K. J. Pena Rodriguez,[50] N. Prouvost,[50] T. Quadfasel,[50] B. Raciti,[50] M. Rieger,[50] D. Savoiu,[50] P. Schleper,[50] M. Schröder,[50] J. Schwandt,[50] M. Sommerhalder,[50] H. Stadie,[50] G. Steinbrück,[50] A. Tews,[50] R. Ward,[50] B. Wiederspan,[50] M. Wolf,[50] S. Brommer,[51] E. Butz,[51] Y. M. Chen,[51] T. Chwalek,[51] A. Dierlamm,[51] G. G. Dincer,[51] U. Elicabuk,[51] N. Faltermann,[51] M. Giffels,[51] A. Gottmann,[51] F. Hartmann,[51,dd] R. Hofsaess,[51] M. Horzela,[51] U. Husemann,[51] J. Kieseler,[51] M. Klute,[51] R. Kunnilan Muhammed Rafeek,[51] O. Lavoryk,[51] J. M. Lawhorn,[51] A. Lintuluoto,[51] S. Maier,[51] M. Mormile,[51] Th. Müller,[51] E. Pfeffer,[51] M. Presilla,[51] G. Quast,[51] K. Rabbertz,[51] B. Regnery,[51] R. Schmieder,[51] N. Shadskiy,[51] I. Shvetsov,[51] H. J. Simonis,[51] L. Sowa,[51] L. Stockmeier,[51] K. Tauqeer,[51] M. Toms,[51] B. Topko,[51] N. Trevisani,[51] C. Verstege,[51] T. Voigtländer,[51] R. F. Von Cube,[51] J. Von Den Driesch,[51] M. Wassmer,[51] R. Wolf,[51] W. D. Zeuner,[51] X. Zuo,[51] G. Anagnostou,[52] G. Daskalakis,[52] A. Kyriakis,[52] G. Melachroinos,[53] Z. Painesis,[53] I. Paraskevas,[53] N. Saoulidou,[53] K. Theofilatos,[53] E. Tziaferi,[53] E. Tzovara,[53] K. Vellidis,[53] I. Zisopoulos,[53] T. Chatzistavrou,[54] G. Karapostoli,[54] K. Kousouris,[54] E. Siamarkou,[54] G. Tsipolitis,[54] I. Bestintzanos,[55] I. Evangelou,[55] C. Foudas,[55] P. Katsoulis,[55] P. Kokkas,[55] P. G. Kosmoglou Kioseoglou,[55] N. Manthos,[55] I. Papadopoulos,[55] J. Strologas,[55] D. Druzhkin,[56] C. Hajdu,[56] D. Horvath,[56,ee,ff] K. Márton,[56] A. J. Rádl,[56,gg] F. Sikler,[56] V. Veszpremi,[56] M. Csanád,[57] K. Farkas,[57] A. Fehérkuti,[57,hh] M. M. A. Gadallah,[57,ii] Á. Kadlecsik,[57] M. León Coello,[57] G. Pásztor,[57] G. I. Veres,[57] B. Ujvari,[58] G. Zilizi,[58] G. Bencze,[59] S. Czellar,[59] J. Molnar,[59] Z. Szillasi,[59] T. Csorgo,[60,hh] F. Nemes,[60,hh] T. Novak,[60] I. Szanyi,[60,jj] S. Bansal,[61] S. B. Beri,[61] V. Bhatnagar,[61] G. Chaudhary,[61] S. Chauhan,[61] N. Dhingra,[61,kk] A. Kaur,[61] A. Kaur,[61] H. Kaur,[61] M. Kaur,[61] S. Kumar,[61] T. Sheokand,[61] J. B. Singh,[61] A. Singla,[61] A. Bhardwaj,[62] A. Chhetri,[62] B. C. Choudhary,[62] A. Kumar,[62] A. Kumar,[62] M. Naimuddin,[62] S. Phor,[62] K. Ranjan,[62] M. K. Saini,[62] S. Acharya,[63,ll] B. Gomber,[63,ll] B. Sahu,[63,ll] S. Mukherjee,[64] S. Baradia,[65] S. Bhattacharya,[65] S. Das Gupta,[65] S. Dutta,[65] S. Dutta,[65] S. Sarkar,[65] M. M. Ameen,[66] P. K. Behera,[66] S. Chatterjee,[66] G. Dash,[66] A. Dattamunsi,[66] P. Jana,[66] P. Kalbhor,[66] S. Kamble,[66] J. R. Komaragiri,[66,mm] T. Mishra,[66] P. R. Pujahari,[66] A. K. Sikdar,[66] R. K. Singh,[66] P. Verma,[66] S. Verma,[66] A. Vijay,[66] B. K. Sirasva,[67] L. Bhatt,[68] S. Dugad,[68] G. B. Mohanty,[68] M. Shelake,[68] P. Suryadevara,[68] A. Bala,[69] S. Banerjee,[69]

S. Barman,[69,nn] R. M. Chatterjee,[69] M. Guchait,[69] Sh. Jain,[69] A. Jaiswal,[69] B. M. Joshi,[69] S. Kumar,[69] M. Maity,[69,nn] G. Majumder,[69] K. Mazumdar,[69] S. Parolia,[69] R. Saxena,[69] A. Thachayath,[69] S. Bahinipati,[70,oo] D. Maity,[70,pp] P. Mal,[70] K. Naskar,[70,pp] A. Nayak,[70,pp] S. Nayak,[70] K. Pal,[70] R. Raturi,[70] P. Sadangi,[70] S. K. Swain,[70] S. Varghese,[70,pp] D. Vats,[70,pp] A. Alpana,[71] S. Dube,[71] P. Hazarika,[71] B. Kansal,[71] A. Laha,[71] R. Sharma,[71] S. Sharma,[71] K. Y. Vaish,[71] S. Ghosh,[72] H. Bakhshiansohi,[73,qq] A. Jafari,[73,rr] V. Sedighzadeh Dalavi,[73] M. Zeinali,[73,ss] S. Bashiri,[74] S. Chenarani,[74,tt] S. M. Etesami,[74] Y. Hosseini,[74] M. Khakzad,[74] E. Khazaie,[74] M. Mohammadi Najafabadi,[74] S. Tizchang,[74,uu] M. Felcini,[75] M. Grunewald,[75] M. Abbrescia,[76a,76b] M. Barbieri,[76a,76b] M. Buonsante,[76a,76b] A. Colaleo,[76a,76b] D. Creanza,[76a,76c] B. D'Anzi,[76a,76b] N. De Filippis,[76a,76c] M. De Palma,[76a,76b] W. Elmetenawee,[76a,76b,r] N. Ferrara,[76a,76c] L. Fiore,[76a] L. Longo,[76a] M. Louka,[76a,76b] G. Maggi,[76a,76c] M. Maggi,[76a] I. Margjeka,[76a] V. Mastrapasqua,[76a,76b] S. My,[76a,76b] F. Nenna,[76a,76b] S. Nuzzo,[76a,76b] A. Pellecchia,[76a,76b] A. Pompili,[76a,76b] G. Pugliese,[76a,76c] R. Radogna,[76a,76b] D. Ramos,[76a] A. Ranieri,[76a] L. Silvestris,[76a] F. M. Simone,[76a,76c] Ü. Sözbilir,[76a] A. Stamerra,[76a,76b] D. Troiano,[76a,76b] R. Venditti,[76a,76b] P. Verwilligen,[76a] A. Zaza,[76a,76b] G. Abbiendi,[77a] C. Battilana,[77a,77b] D. Bonacorsi,[77a,77b] P. Capiluppi,[77a,77b] F. R. Cavallo,[77a] M. Cuffiani,[77a,77b] G. M. Dallavalle,[77a] T. Diotalevi,[77a,77b] F. Fabbri,[77a] A. Fanfani,[77a,77b] D. Fasanella,[77a] P. Giacomelli,[77a] C. Grandi,[77a] L. Guiducci,[77a,77b] S. Lo Meo,[77a,vv] M. Lorusso,[77a,77b] L. Lunerti,[77a] S. Marcellini,[77a] G. Masetti,[77a] F. L. Navarria,[77a,77b] G. Paggi,[77a,77b] A. Perrotta,[77a] F. Primavera,[77a,77b] A. M. Rossi,[77a,77b] S. Rossi Tisbeni,[77a,77b] T. Rovelli,[77a,77b] S. Costa,[78a,78b,ww] A. Di Mattia,[78a] A. Lapertosa,[78a] R. Potenza,[78a,78b] A. Tricomi,[78a,78b,ww] J. Altork,[79a,79b] P. Assiouras,[79a] G. Barbagli,[79a] G. Bardelli,[79a] M. Bartolini,[79a,79b] A. Calandri,[79a,79b] B. Camaiani,[79a,79b] A. Cassese,[79a] R. Ceccarelli,[79a] V. Ciulli,[79a,79b] C. Civinini,[79a] R. D'Alessandro,[79a,79b] L. Damenti,[79a,79b] E. Focardi,[79a,79b] T. Kello,[79a] G. Latino,[79a,79b] P. Lenzi,[79a,79b] M. Lizzo,[79a] M. Meschini,[79a] S. Paoletti,[79a] A. Papanastassiou,[79a,79b] G. Sguazzoni,[79a] L. Viliani,[79a] L. Benussi,[80] S. Colafranceschi,[80,xx] S. Meola,[80,yy] D. Piccolo,[80] M. Alves Gallo Pereira,[81a] F. Ferro,[81a] E. Robutti,[81a] S. Tosi,[81a,81b] A. Benaglia,[82a] F. Brivio,[82a] V. Camagni,[82a,82b] F. Cetorelli,[82a,82b] F. De Guio,[82a,82b] M. E. Dinardo,[82a,82b] P. Dini,[82a] S. Gennai,[82a] R. Gerosa,[82a,82b] A. Ghezzi,[82a,82b] P. Govoni,[82a,82b] L. Guzzi,[82a] M. R. Kim,[82a] G. Lavizzari,[82a,82b] M. T. Lucchini,[82a,82b] M. Malberti,[82a] S. Malvezzi,[82a] A. Massironi,[82a] D. Menasce,[82a] L. Moroni,[82a] M. Paganoni,[82a,82b] S. Palluotto,[82a,82b] D. Pedrini,[82a] A. Perego,[82a,82b] B. S. Pinolini,[82a] G. Pizzati,[82a,82b] S. Ragazzi,[82a,82b] T. Tabarelli de Fatis,[82a,82b] S. Buontempo,[83a] C. Di Fraia,[83a,83b] F. Fabozzi,[83a,83c] L. Favilla,[83a,83d] A. O. M. Iorio,[83a,83b] L. Lista,[83a,83b,zz] P. Paolucci,[83a,dd] B. Rossi,[83a] P. Azzi,[84a] N. Bacchetta,[84a,aaa] M. Benettoni,[84a] D. Bisello,[84a,84b] P. Bortignon,[84a,84c] G. Bortolato,[84a,84b] A. C. M. Bulla,[84a,84c] R. Carlin,[84a,84b] P. Checchia,[84a] T. Dorigo,[84a,bbb] F. Gasparini,[84a,84b] U. Gasparini,[84a,84b] S. Giorgetti,[84a] E. Lusiani,[84a] M. Margoni,[84a,84b] J. Pazzini,[84a,84b] P. Ronchese,[84a,84b] R. Rossin,[84a,84b] F. Simonetto,[84a,84b] M. Tosi,[84a,84b] A. Triossi,[84a,84b] S. Ventura,[84a] P. Zotto,[84a,84b] A. Zucchetta,[84a,84b] G. Zumerle,[84a,84b] A. Braghieri,[85a] S. Calzaferri,[85a] P. Montagna,[85a,85b] M. Pelliccioni,[85a] V. Re,[85a] C. Riccardi,[85a,85b] P. Salvini,[85a] I. Vai,[85a,85b] P. Vitulo,[85a,85b] S. Ajmal,[86a,86b] M. E. Ascioti,[86a,86b] G. M. Bilei,[86a] C. Carrivale,[86a,86b] D. Ciangottini,[86a,86b] L. Della Penna,[86a,86b] L. Fanò,[86a,86b] V. Mariani,[86a,86b] M. Menichelli,[86a] F. Moscatelli,[86a,ccc] A. Rossi,[86a,86b] A. Santocchia,[86a,86b] D. Spiga,[86a] T. Tedeschi,[86a,86b] C. Aimè,[87a,87b] C. A. Alexe,[87a,87c] P. Asenov,[87a,87b] P. Azzurri,[87a] G. Bagliesi,[87a] R. Bhattacharya,[87a] L. Bianchini,[87a,87b] T. Boccali,[87a] E. Bossini,[87a] D. Bruschini,[87a,87c] L. Calligaris,[87a,87b] R. Castaldi,[87a] F. Cattafesta,[87a,87c] M. A. Ciocci,[87a,87d] M. Cipriani,[87a,87b] R. Dell'Orso,[87a] S. Donato,[87a,87b] R. Forti,[87a,87b] A. Giassi,[87a] F. Ligabue,[87a,87c] A. C. Marini,[87a,87b] D. Matos Figueiredo,[87a] A. Messineo,[87a,87b] S. Mishra,[87a] V. K. Muraleedharan Nair Bindhu,[87a,87b] S. Nandan,[87a] F. Palla,[87a] M. Riggirello,[87a,87c] A. Rizzi,[87a,87b] G. Rolandi,[87a,87c] S. Roy Chowdhury,[87a,ddd] T. Sarkar,[87a] A. Scribano,[87a] P. Solanki,[87a,87b] P. Spagnolo,[87a] F. Tenchini,[87a,87b] R. Tenchini,[87a] G. Tonelli,[87a,87b] N. Turini,[87a,87d] F. Vaselli,[87a,87c] A. Venturi,[87a] P. G. Verdini,[87a] P. Akrap,[88a,88b] C. Basile,[88a,88b] S. C. Behera,[88a] F. Cavallari,[88a] L. Cunqueiro Mendez,[88a,88b] F. De Riggi,[88a,88b] D. Del Re,[88a,88b] E. Di Marco,[88a] F. Errico,[88a] L. Frosina,[88a,88b] R. Gargiulo,[88a,88b] B. Harikrishnan,[88a,88b] F. Lombardi,[88a,88b] E. Longo,[88a,88b] L. Martikainen,[88a,88b] J. Mijuskovic,[88a,88b] G. Organtini,[88a,88b] N. Palmeri,[88a,88b] F. Pandolfi,[88a] R. Paramatti,[88a,88b] C. Quaranta,[88a,88b] S. Rahatlou,[88a,88b] C. Rovelli,[88a] F. Santanastasio,[88a,88b] L. Soffi,[88a] V. Vladimirov,[88a,88b] N. Amapane,[89a,89b] R. Arcidiacono,[89a,89c] S. Argiro,[89a,89b] M. Arneodo,[89a,89c] N. Bartosik,[89a,89c] R. Bellan,[89a,89b] A. Bellora,[89a,89b]

C. Biino,[89a] C. Borca,[89a,89b] N. Cartiglia,[89a] M. Costa,[89a,89b] R. Covarelli,[89a,89b] N. Demaria,[89a] L. Finco,[89a] M. Grippo,[89a,89b] B. Kiani,[89a,89b] L. Lanteri,[89a,89b] F. Legger,[89a] F. Luongo,[89a,89b] C. Mariotti,[89a] S. Maselli,[89a] A. Mecca,[89a,89b] L. Menzio,[89a,89b] P. Meridiani,[89a] E. Migliore,[89a,89b] M. Monteno,[89a] M. M. Obertino,[89a,89b] G. Ortona,[89a] L. Pacher,[89a,89b] N. Pastrone,[89a] M. Ruspa,[89a,89c] F. Siviero,[89a,89b] V. Sola,[89a,89b] A. Solano,[89a,89b] A. Staiano,[89a] C. Tarricone,[89a,89b] D. Trocino,[89a] G. Umoret,[89a,89b] E. Vlasov,[89a,89b] R. White,[89a,89b] J. Babbar,[90a,90b] S. Belforte,[90a] V. Candelise,[90a,90b] M. Casarsa,[90a] F. Cossutti,[90a] K. De Leo,[90a] G. Della Ricca,[90a,90b] R. Delli Gatti,[90a,90b] S. Dogra,[91] J. Hong,[91] J. Kim,[91] T. Kim,[91] D. Lee,[91] H. Lee,[91] J. Lee,[91] S. W. Lee,[91] C. S. Moon,[91] Y. D. Oh,[91] S. Sekmen,[91] B. Tae,[91] Y. C. Yang,[91] M. S. Kim,[92] G. Bak,[93] P. Gwak,[93] H. Kim,[93] D. H. Moon,[93] J. Seo,[93] E. Asilar,[94] F. Carnevali,[94] J. Choi,[94,eee] T. J. Kim,[94] Y. Ryou,[94] S. Ha,[95] S. Han,[95] B. Hong,[95] J. Kim,[95] K. Lee,[95] K. S. Lee,[95] S. Lee,[95] J. Yoo,[95] J. Goh,[96] J. Shin,[96] S. Yang,[96] Y. Kang,[97] H. S. Kim,[97] Y. Kim,[97] S. Lee,[97] J. Almond,[98] J. H. Bhyun,[98] J. Choi,[98] J. Choi,[98] W. Jun,[98] H. Kim,[98] J. Kim,[98] T. Kim,[98] Y. Kim,[98] Y. W. Kim,[98] S. Ko,[98] H. Lee,[98] J. Lee,[98] J. Lee,[98] B. H. Oh,[98] S. B. Oh,[98] J. Shin,[98] U. K. Yang,[98] I. Yoon,[98] W. Jang,[99] D. Y. Kang,[99] D. Kim,[99] S. Kim,[99] B. Ko,[99] J. S. H. Lee,[99] Y. Lee,[99] I. C. Park,[99] Y. Roh,[99] I. J. Watson,[99] G. Cho,[100] K. Hwang,[100] B. Kim,[100] S. Kim,[100] K. Lee,[100] H. D. Yoo,[100] M. Choi,[101] Y. Lee,[101] I. Yu,[101] T. Beyrouthy,[102] Y. Gharbia,[102] F. Alazemi,[103] K. Dreimanis,[104] O. M. Eberlins,[104] A. Gaile,[104] C. Munoz Diaz,[104] D. Osite,[104] G. Pikurs,[104] R. Plese,[104] A. Potrebko,[104] M. Seidel,[104] D. Sidiropoulos Kontos,[104] N. R. Strautnieks,[105] M. Ambrozas,[106] A. Juodagalvis,[106] S. Nargelas,[106] A. Rinkevicius,[106] G. Tamulaitis,[106] I. Yusuff,[107,fff] Z. Zolkapli,[107] J. F. Benitez,[108] A. Castaneda Hernandez,[108] A. Cota Rodriguez,[108] L. E. Cuevas Picos,[108] H. A. Encinas Acosta,[108] L. G. Gallegos Maríñez,[108] J. A. Murillo Quijada,[108] A. Sehrawat,[108] L. Valencia Palomo,[108] G. Ayala,[109] H. Castilla-Valdez,[109] H. Crotte Ledesma,[109] R. Lopez-Fernandez,[109] J. Mejia Guisao,[109] R. Reyes-Almanza,[109] A. Sánchez Hernández,[109] C. Oropeza Barrera,[110] D. L. Ramirez Guadarrama,[110] M. Ramírez García,[110] I. Bautista,[111] F. E. Neri Huerta,[111] I. Pedraza,[111] H. A. Salazar Ibarguen,[111] C. Uribe Estrada,[111] I. Bubanja,[112] N. Raicevic,[112] P. H. Butler,[113] A. Ahmad,[114] M. I. Asghar,[114] A. Awais,[114] M. I. M. Awan,[114] W. A. Khan,[114] V. Avati,[115] L. Forthomme,[115] L. Grzanka,[115] M. Malawski,[115] K. Piotrzkowski,[115] M. Bluj,[116] M. Górski,[116] M. Kazana,[116] M. Szleper,[116] P. Zalewski,[116] K. Bunkowski,[117] K. Doroba,[117] A. Kalinowski,[117] M. Konecki,[117] J. Krolikowski,[117] A. Muhammad,[117] P. Fokow,[118] K. Pozniak,[118] W. Zabolotny,[118] M. Araujo,[119] D. Bastos,[119] C. Beirão Da Cruz E Silva,[119] A. Boletti,[119] M. Bozzo,[119] T. Camporesi,[119] G. Da Molin,[119] M. Gallinaro,[119] J. Hollar,[119] N. Leonardo,[119] G. B. Marozzo,[119] A. Petrilli,[119] M. Pisano,[119] J. Seixas,[119] J. Varela,[119] J. W. Wulff,[119] P. Adzic,[120] L. Markovic,[120] P. Milenovic,[120] V. Milosevic,[120] D. Devetak,[121] M. Dordevic,[121] J. Milosevic,[121] L. Nadderd,[121] V. Rekovic,[121] M. Stojanovic,[121] M. Alcalde Martinez,[122] J. Alcaraz Maestre,[122] Cristina F. Bedoya,[122] J. A. Brochero Cifuentes,[122] Oliver M. Carretero,[122] M. Cepeda,[122] M. Cerrada,[122] N. Colino,[122] J. Cuchillo Ortega,[122] B. De La Cruz,[122] A. Delgado Peris,[122] A. Escalante Del Valle,[122] D. Fernández Del Val,[122] J. P. Fernández Ramos,[122] J. Flix,[122] M. C. Fouz,[122] M. Gonzalez Hernandez,[122] O. Gonzalez Lopez,[122] S. Goy Lopez,[122] J. M. Hernandez,[122] M. I. Josa,[122] J. Llorente Merino,[122] C. Martin Perez,[122] E. Martin Viscasillas,[122] D. Moran,[122] C. M. Morcillo Perez,[122] R. Paz Herrera,[122] C. Perez Dengra,[122] A. Pérez-Calero Yzquierdo,[122] J. Puerta Pelayo,[122] I. Redondo,[122] J. Vazquez Escobar,[122] J. F. de Trocóniz,[123] B. Alvarez Gonzalez,[124] J. Ayllon Torresano,[124] A. Cardini,[124] J. Cuevas,[124] J. Del Riego Badas,[124] D. Estrada Acevedo,[124] J. Fernandez Menendez,[124] S. Folgueras,[124] I. Gonzalez Caballero,[124] P. Leguina,[124] M. Obeso Menendez,[124] E. Palencia Cortezon,[124] J. Prado Pico,[124] A. Soto Rodríguez,[124] C. Vico Villalba,[124] P. Vischia,[124] S. Blanco Fernández,[125] I. J. Cabrillo,[125] A. Calderon,[125] J. Duarte Campderros,[125] M. Fernandez,[125] G. Gomez,[125] C. Lasaosa García,[125] R. Lopez Ruiz,[125] C. Martinez Rivero,[125] P. Martinez Ruiz del Arbol,[125] F. Matorras,[125] P. Matorras Cuevas,[125] E. Navarrete Ramos,[125] J. Piedra Gomez,[125] C. Quintana San Emeterio,[125] L. Scodellaro,[125] I. Vila,[125] R. Vilar Cortabitarte,[125] J. M. Vizan Garcia,[125] B. Kailasapathy,[126,ggg] D. D. C. Wickramarathna,[126] W. G. D. Dharmaratna,[127,hhh] K. Liyanage,[127] N. Perera,[127] D. Abbaneo,[128] C. Amendola,[128] R. Ardino,[128] E. Auffray,[128] J. Baechler,[128] D. Barney,[128] M. Bianco,[128] A. Bocci,[128] L. Borgonovi,[128] C. Botta,[128] A. Bragagnolo,[128] C. E. Brown,[128] C. Caillol,[128] G. Cerminara,[128] P. Connor,[128] D. d'Enterria,[128] A. Dabrowski,[128] A. David,[128] A. De Roeck,[128] M. M. Defranchis,[128] M. Deile,[128] M. Dobson,[128]

P. J. Fernández Manteca,[128] W. Funk,[128] A. Gaddi,[128] S. Giani,[128] D. Gigi,[128] K. Gill,[128] F. Glege,[128] M. Glowacki,[128] A. Gruber,[128] J. Hegeman,[128] J. K. Heikkilä,[128] B. Huber,[128] V. Innocente,[128] T. James,[128] P. Janot,[128] O. Kaluzinska,[128] O. Karacheban,[128,bb] G. Karathanasis,[128] S. Laurila,[128] P. Lecoq,[128] C. Lourenço,[128] A.-M. Lyon,[128] M. Magherini,[128] L. Malgeri,[128] M. Mannelli,[128] A. Mehta,[128] F. Meijers,[128] J. A. Merlin,[128] S. Mersi,[128] E. Meschi,[128] M. Migliorini,[128] F. Monti,[128] F. Moortgat,[128] M. Mulders,[128] M. Musich,[128] I. Neutelings,[128] S. Orfanelli,[128] F. Pantaleo,[128] M. Pari,[128] G. Petrucciani,[128] A. Pfeiffer,[128] M. Pierini,[128] M. Pitt,[128] H. Qu,[128] D. Rabady,[128] A. Reimers,[128] B. Ribeiro Lopes,[128] F. Riti,[128] P. Rosado,[128] M. Rovere,[128] H. Sakulin,[128] R. Salvatico,[128] S. Sanchez Cruz,[128] S. Scarfi,[128] M. Selvaggi,[128] A. Sharma,[128] K. Shchelina,[128] P. Silva,[128] P. Sphicas,[128,iii] A. G. Stahl Leiton,[128] A. Steen,[128] S. Summers,[128] D. Treille,[128] P. Tropea,[128] E. Vernazza,[128] J. Wanczyk,[128,jjj] J. Wang,[128] S. Wuchterl,[128] M. Zarucki,[128] P. Zehetner,[128] P. Zejdl,[128] G. Zevi Della Porta,[128] T. Bevilacqua,[129,kkk] L. Caminada,[129,kkk] W. Erdmann,[129] R. Horisberger,[129] Q. Ingram,[129] H. C. Kaestli,[129] D. Kotlinski,[129] C. Lange,[129] U. Langenegger,[129] M. Missiroli,[129,kkk] L. Noehte,[129,kkk] T. Rohe,[129] A. Samalan,[129] T. K. Aarrestad,[130] M. Backhaus,[130] G. Bonomelli,[130] C. Cazzaniga,[130] K. Datta,[130] P. De Bryas Dexmiers D'archiacchiac,[130,jjj] A. De Cosa,[130] G. Dissertori,[130] M. Dittmar,[130] M. Donegà,[130] F. Eble,[130] K. Gedia,[130] F. Glessgen,[130] C. Grab,[130] N. Härringer,[130] T. G. Harte,[130] W. Lustermann,[130] M. Malucchi,[130] R. A. Manzoni,[130] M. Marchegiani,[130] L. Marchese,[130] A. Mascellani,[130,jjj] F. Nessi-Tedaldi,[130] F. Pauss,[130] V. Perovic,[130] B. Ristic,[130] R. Seidita,[130] J. Steggemann,[130,jjj] A. Tarabini,[130] D. Valsecchi,[130] R. Wallny,[130] C. Amsler,[131,lll] P. Bärtschi,[131] F. Bilandzija,[131] M. F. Canelli,[131] G. Celotto,[131] K. Cormier,[131] M. Huwiler,[131] W. Jin,[131] A. Jofrehei,[131] B. Kilminster,[131] T. H. Kwok,[131] S. Leontsinis,[131] V. Lukashenko,[131] A. Macchiolo,[131] F. Meng,[131] J. Motta,[131] P. Robmann,[131] M. Senger,[131] E. Shokr,[131] F. Stäger,[131] R. Tramontano,[131] D. Bhowmik,[132] C. M. Kuo,[132] P. K. Rout,[132] S. Taj,[132] P. C. Tiwari,[132,mm] L. Ceard,[133] K. F. Chen,[133] Z. g. Chen,[133] A. De Iorio,[133] W.-S. Hou,[133] T. h. Hsu,[133] Y. w. Kao,[133] S. Karmakar,[133] G. Kole,[133] Y. y. Li,[133] R.-S. Lu,[133] E. Paganis,[133] X. f. Su,[133] J. Thomas-Wilsker,[133] L. s. Tsai,[133] D. Tsionou,[133] H. y. Wu,[133] E. Yazgan,[133] C. Asawatangtrakuldee,[134] N. Srimanobhas,[134] Y. Maghrbi,[135] D. Agyel,[136] F. Dolek,[136] I. Dumanoglu,[136,mmm] Y. Guler,[136,nnn] E. Gurpinar Guler,[136,nnn] C. Isik,[136] O. Kara,[136] A. Kayis Topaksu,[136] Y. Komurcu,[136] G. Onengut,[136] K. Ozdemir,[136,ooo] B. Tali,[136,ppp] U. G. Tok,[136] E. Uslan,[136] I. S. Zorbakir,[136] M. Yalvac,[137,qqq] B. Akgun,[138] I. O. Atakisi,[138,rrr] E. Gülmez,[138] M. Kaya,[138,sss] O. Kaya,[138,ttt] M. A. Sarkisla,[138,uuu] S. Tekten,[138,vvv] A. Cakir,[139] K. Cankocak,[139,mmm,www] S. Sen,[139,xxx] O. Aydilek,[140,yyy] B. Hacisahinoglu,[140] I. Hos,[140,zzz] B. Kaynak,[140] S. Ozkorucuklu,[140] O. Potok,[140] H. Sert,[140] C. Simsek,[140] C. Zorbilmez,[140] S. Cerci,[141] B. Isildak,[141,aaaa] E. Simsek,[141] D. Sunar Cerci,[141] T. Yetkin,[141,w] A. Boyaryntsev,[142] O. Dadazhanova,[142] B. Grynyov,[142] L. Levchuk,[143] J. J. Brooke,[144] A. Bundock,[144] F. Bury,[144] E. Clement,[144] D. Cussans,[144] D. Dharmender,[144] H. Flacher,[144] J. Goldstein,[144] H. F. Heath,[144] M.-L. Holmberg,[144] L. Kreczko,[144] S. Paramesvaran,[144] L. Robertshaw,[144] M. S. Sanjrani,[144,qq] J. Segal,[144] V. J. Smith,[144] A. H. Ball,[145] K. W. Bell,[145] A. Belyaev,[145,bbbb] C. Brew,[145] R. M. Brown,[145] D. J. A. Cockerill,[145] A. Elliot,[145] K. V. Ellis,[145] J. Gajownik,[145] K. Harder,[145] S. Harper,[145] J. Linacre,[145] K. Manolopoulos,[145] M. Moallemi,[145] D. M. Newbold,[145] E. Olaiya,[145] D. Petyt,[145] T. Reis,[145] A. R. Sahasransu,[145] G. Salvi,[145] T. Schuh,[145] C. H. Shepherd-Themistocleous,[145] I. R. Tomalin,[145] K. C. Whalen,[145] T. Williams,[145] I. Andreou,[146] R. Bainbridge,[146] P. Bloch,[146] O. Buchmuller,[146] C. A. Carrillo Montoya,[146] D. Colling,[146] J. S. Dancu,[146] I. Das,[146] P. Dauncey,[146] G. Davies,[146] M. Della Negra,[146] S. Fayer,[146] G. Fedi,[146] G. Hall,[146] H. R. Hoorani,[146] A. Howard,[146] G. Iles,[146] C. R. Knight,[146] P. Krueper,[146] J. Langford,[146] K. H. Law,[146] J. León Holgado,[146] E. Leutgeb,[146] L. Lyons,[146] A.-M. Magnan,[146] B. Maier,[146] S. Mallios,[146] A. Mastronikolis,[146] M. Mieskolainen,[146] J. Nash,[146,cccc] M. Pesaresi,[146] P. B. Pradeep,[146] B. C. Radburn-Smith,[146] A. Richards,[146] A. Rose,[146] L. Russell,[146] K. Savva,[146] C. Seez,[146] R. Shukla,[146] A. Tapper,[146] K. Uchida,[146] G. P. Uttley,[146] T. Virdee,[146,dd] M. Vojinovic,[146] N. Wardle,[146] D. Winterbottom,[146] J. E. Cole,[147] A. Khan,[147] P. Kyberd,[147] I. D. Reid,[147] S. Abdullin,[148] A. Brinkerhoff,[148] E. Collins,[148] M. R. Darwish,[148] J. Dittmann,[148] K. Hatakeyama,[148] V. Hegde,[148] J. Hiltbrand,[148] B. McMaster,[148] J. Samudio,[148] S. Sawant,[148] C. Sutantawibul,[148] J. Wilson,[148] J. M. Hogan,[149,dddd] R. Bartek,[150] A. Dominguez,[150] S. Raj,[150] A. E. Simsek,[150] S. S. Yu,[150] B. Bam,[151] A. Buchot Perraguin,[151] S. Campbell,[151] R. Chudasama,[151] S. I. Cooper,[151] C. Crovella,[151] G. Fidalgo,[151] S. V. Gleyzer,[151] A. Khukhunaishvili,[151] K. Matchev,[151]

E. Pearson,[151] C. U. Perez,[151] P. Rumerio,[151,eeee] E. Usai,[151] R. Yi,[151] S. Cholak,[152] G. De Castro,[152] Z. Demiragli,[152] C. Erice,[152] C. Fangmeier,[152] C. Fernandez Madrazo,[152] E. Fontanesi,[152] J. Fulcher,[152] F. Golf,[152] S. Jeon,[152] J. O'Cain,[152] I. Reed,[152] J. Rohlf,[152] K. Salyer,[152] D. Sperka,[152] D. Spitzbart,[152] I. Suarez,[152] A. Tsatsos,[152] E. Wurtz,[152] A. G. Zecchinelli,[152] G. Barone,[153] G. Benelli,[153] D. Cutts,[153] S. Ellis,[153] L. Gouskos,[153] M. Hadley,[153] U. Heintz,[153] K. W. Ho,[153] T. Kwon,[153] G. Landsberg,[153] K. T. Lau,[153] J. Luo,[153] S. Mondal,[153] J. Roloff,[153] T. Russell,[153] S. Sagir,[153,ffff] X. Shen,[153] M. Stamenkovic,[153] N. Venkatasubramanian,[153] S. Abbott,[154] B. Barton,[154] R. Breedon,[154] H. Cai,[154] M. Calderon De La Barca Sanchez,[154] M. Chertok,[154] M. Citron,[154] J. Conway,[154] P. T. Cox,[154] R. Erbacher,[154] O. Kukral,[154] G. Mocellin,[154] S. Ostrom,[154] I. Salazar Segovia,[154] W. Wei,[154] S. Yoo,[154] K. Adamidis,[155] M. Bachtis,[155] D. Campos,[155] R. Cousins,[155] A. Datta,[155] G. Flores Avila,[155] J. Hauser,[155] M. Ignatenko,[155] M. A. Iqbal,[155] T. Lam,[155] Y. f. Lo,[155] E. Manca,[155] A. Nunez Del Prado,[155] D. Saltzberg,[155] V. Valuev,[155] R. Clare,[156] J. W. Gary,[156] G. Hanson,[156] A. Aportela,[157] A. Arora,[157] J. G. Branson,[157] S. Cittolin,[157] S. Cooperstein,[157] D. Diaz,[157] J. Duarte,[157] L. Giannini,[157] Y. Gu,[157] J. Guiang,[157] V. Krutelyov,[157] R. Lee,[157] J. Letts,[157] H. Li,[157] M. Masciovecchio,[157] F. Mokhtar,[157] S. Mukherjee,[157] M. Pieri,[157] D. Primosch,[157] M. Quinnan,[157] V. Sharma,[157] M. Tadel,[157] E. Vourliotis,[157] F. Würthwein,[157] A. Yagil,[157] Z. Zhao,[157] A. Barzdukas,[158] L. Brennan,[158] C. Campagnari,[158] S. Carron Montero,[158,gggg] K. Downham,[158] C. Grieco,[158] M. M. Hussain,[158] J. Incandela,[158] M. W. K. Lai,[158] A. J. Li,[158] P. Masterson,[158] J. Richman,[158] S. N. Santpur,[158] U. Sarica,[158] R. Schmitz,[158] F. Setti,[158] J. Sheplock,[158] D. Stuart,[158] T. Á. Vámi,[158] X. Yan,[158] D. Zhang,[158] A. Albert,[159] S. Bhattacharya,[159] A. Bornheim,[159] O. Cerri,[159] R. Kansal,[159] J. Mao,[159] H. B. Newman,[159] G. Reales Gutiérrez,[159] T. Sievert,[159] M. Spiropulu,[159] J. R. Vlimant,[159] R. A. Wynne,[159] S. Xie,[159] J. Alison,[160] S. An,[160] M. Cremonesi,[160] V. Dutta,[160] E. Y. Ertorer,[160] T. Ferguson,[160] T. A. Gómez Espinosa,[160] A. Harilal,[160] A. Kallil Tharayil,[160] M. Kanemura,[160] C. Liu,[160] P. Meiring,[160] T. Mudholkar,[160] S. Murthy,[160] P. Palit,[160] K. Park,[160] M. Paulini,[160] A. Roberts,[160] A. Sanchez,[160] W. Terrill,[160] J. P. Cumalat,[161] W. T. Ford,[161] A. Hart,[161] A. Hassani,[161] S. Kwan,[161] J. Pearkes,[161] C. Savard,[161] N. Schonbeck,[161] K. Stenson,[161] K. A. Ulmer,[161] S. R. Wagner,[161] N. Zipper,[161] D. Zuolo,[161] J. Alexander,[162] X. Chen,[162] D. J. Cranshaw,[162] J. Dickinson,[162] J. Fan,[162] X. Fan,[162] J. Grassi,[162] S. Hogan,[162] P. Kotamnives,[162] J. Monroy,[162] G. Niendorf,[162] M. Oshiro,[162] J. R. Patterson,[162] M. Reid,[162] A. Ryd,[162] J. Thom,[162] P. Wittich,[162] R. Zou,[162] L. Zygala,[162] M. Albrow,[163] M. Alyari,[163] O. Amram,[163] G. Apollinari,[163] A. Apresyan,[163] L. A. T. Bauerdick,[163] D. Berry,[163] J. Berryhill,[163] P. C. Bhat,[163] K. Burkett,[163] J. N. Butler,[163] A. Canepa,[163] G. B. Cerati,[163] H. W. K. Cheung,[163] F. Chlebana,[163] C. Cosby,[163] G. Cummings,[163] I. Dutta,[163] V. D. Elvira,[163] J. Freeman,[163] A. Gandrakota,[163] Z. Gecse,[163] L. Gray,[163] D. Green,[163] A. Grummer,[163] S. Grünendahl,[163] D. Guerrero,[163] O. Gutsche,[163] R. M. Harris,[163] T. C. Herwig,[163] J. Hirschauer,[163] B. Jayatilaka,[163] S. Jindariani,[163] M. Johnson,[163] U. Joshi,[163] T. Klijnsma,[163] B. Klima,[163] K. H. M. Kwok,[163] S. Lammel,[163] C. Lee,[163] D. Lincoln,[163] R. Lipton,[163] T. Liu,[163] K. Maeshima,[163] D. Mason,[163] P. McBride,[163] P. Merkel,[163] S. Mrenna,[163] S. Nahn,[163] J. Ngadiuba,[163] D. Noonan,[163] S. Norberg,[163] V. Papadimitriou,[163] N. Pastika,[163] K. Pedro,[163] C. Pena,[163,hhhh] C. E. Perez Lara,[163] F. Ravera,[163] A. Reinsvold Hall,[163,iiii] L. Ristori,[163] M. Safdari,[163] E. Sexton-Kennedy,[163] N. Smith,[163] A. Soha,[163] L. Spiegel,[163] S. Stoynev,[163] J. Strait,[163] L. Taylor,[163] S. Tkaczyk,[163] N. V. Tran,[163] L. Uplegger,[163] E. W. Vaandering,[163] C. Wang,[163] I. Zoi,[163] C. Aruta,[164] P. Avery,[164] D. Bourilkov,[164] P. Chang,[164] V. Cherepanov,[164] R. D. Field,[164] C. Huh,[164] E. Koenig,[164] M. Kolosova,[164] J. Konigsberg,[164] A. Korytov,[164] N. Menendez,[164] G. Mitselmakher,[164] K. Mohrman,[164] A. Muthirakalayil Madhu,[164] N. Rawal,[164] S. Rosenzweig,[164] V. Sulimov,[164] Y. Takahashi,[164] J. Wang,[164] T. Adams,[165] A. Al Kadhim,[165] A. Askew,[165] S. Bower,[165] R. Hashmi,[165] R. S. Kim,[165] T. Kolberg,[165] G. Martinez,[165] M. Mazza,[165] H. Prosper,[165] P. R. Prova,[165] M. Wulansatiti,[165] R. Yohay,[165] B. Alsufyani,[166] S. Butalla,[166] S. Das,[166] M. Hohlmann,[166] M. Lavinsky,[166] E. Yanes,[166] M. R. Adams,[167] N. Barnett,[167] A. Baty,[167] C. Bennett,[167] R. Cavanaugh,[167] R. Escobar Franco,[167] O. Evdokimov,[167] C. E. Gerber,[167] H. Gupta,[167] M. Hawksworth,[167] A. Hingrajiya,[167] D. J. Hofman,[167] J. h. Lee,[167] D. S. Lemos,[167] C. Mills,[167] S. Nanda,[167] G. Nigmatkulov,[167] B. Ozek,[167] T. Phan,[167] D. Pilipovic,[167] R. Pradhan,[167] E. Prifti,[167] P. Roy,[167] T. Roy,[167] N. Singh,[167] M. B. Tonjes,[167] N. Varelas,[167] M. A. Wadud,[167] J. Yoo,[167] M. Alhusseini,[168] D. Blend,[168] K. Dilsiz,[168,jjjj] O. K. Köseyan,[168] A. Mestvirishvili,[168,kkkk] O. Neogi,[168] H. Ogul,[168,llll] Y. Onel,[168]

A. Penzo,[168] C. Snyder,[168] E. Tiras,[168,mmmm] B. Blumenfeld,[169] J. Davis,[169] A. V. Gritsan,[169] L. Kang,[169] S. Kyriacou,[169] P. Maksimovic,[169] M. Roguljic,[169] S. Sekhar,[169] M. V. Srivastav,[169] M. Swartz,[169] A. Abreu,[170] L. F. Alcerro Alcerro,[170] J. Anguiano,[170] S. Arteaga Escatel,[170] P. Baringer,[170] A. Bean,[170] Z. Flowers,[170] D. Grove,[170] J. King,[170] G. Krintiras,[170] M. Lazarovits,[170] C. Le Mahieu,[170] J. Marquez,[170] M. Murray,[170] M. Nickel,[170] S. Popescu,[170,nnnn] C. Rogan,[170] C. Royon,[170] S. Rudrabhatla,[170] S. Sanders,[170] C. Smith,[170] G. Wilson,[170] B. Allmond,[171] N. Islam,[171] A. Ivanov,[171] K. Kaadze,[171] Y. Maravin,[171] J. Natoli,[171] G. G. Reddy,[171] D. Roy,[171] G. Sorrentino,[171] A. Baden,[172] A. Belloni,[172] J. Bistany-riebman,[172] S. C. Eno,[172] N. J. Hadley,[172] S. Jabeen,[172] R. G. Kellogg,[172] T. Koeth,[172] B. Kronheim,[172] S. Lascio,[172] P. Major,[172] A. C. Mignerey,[172] C. Palmer,[172] C. Papageorgakis,[172] M. M. Paranjpe,[172] E. Popova,[172,oooo] A. Shevelev,[172] L. Zhang,[172] C. Baldenegro Barrera,[173] J. Bendavid,[173] H. Bossi,[173] S. Bright-Thonney,[173] I. A. Cali,[173] Y. c. Chen,[173] P. c. Chou,[173] M. D'Alfonso,[173] J. Eysermans,[173] C. Freer,[173] G. Gomez-Ceballos,[173] M. Goncharov,[173] G. Grosso,[173] P. Harris,[173] D. Hoang,[173] G. M. Innocenti,[173] D. Kovalskyi,[173] J. Krupa,[173] L. Lavezzo,[173] Y.-J. Lee,[173] K. Long,[173] C. Mcginn,[173] A. Novak,[173] M. I. Park,[173] C. Paus,[173] C. Reissel,[173] C. Roland,[173] G. Roland,[173] S. Rothman,[173] T. a. Sheng,[173] G. S. F. Stephans,[173] D. Walter,[173] Z. Wang,[173] B. Wyslouch,[173] T. J. Yang,[173] B. Crossman,[174] W. J. Jackson,[174] C. Kapsiak,[174] M. Krohn,[174] D. Mahon,[174] J. Mans,[174] B. Marzocchi,[174] R. Rusack,[174] O. Sancar,[174] R. Saradhy,[174] N. Strobbe,[174] K. Bloom,[175] D. R. Claes,[175] G. Haza,[175] J. Hossain,[175] C. Joo,[175] I. Kravchenko,[175] A. Rohilla,[175] J. E. Siado,[175] W. Tabb,[175] A. Vagnerini,[175] A. Wightman,[175] F. Yan,[175] H. Bandyopadhyay,[176] L. Hay,[176] H. w. Hsia,[176] I. Iashvili,[176] A. Kalogeropoulos,[176] A. Kharchilava,[176] A. Mandal,[176] M. Morris,[176] D. Nguyen,[176] S. Rappoccio,[176] H. Rejeb Sfar,[176] A. Williams,[176] P. Young,[176] D. Yu,[176] G. Alverson,[177] E. Barberis,[177] J. Bonilla,[177] B. Bylsma,[177] M. Campana,[177] J. Dervan,[177] Y. Haddad,[177] Y. Han,[177] I. Israr,[177] A. Krishna,[177] M. Lu,[177] N. Manganelli,[177] R. Mccarthy,[177] D. M. Morse,[177] T. Orimoto,[177] A. Parker,[177] L. Skinnari,[177] C. S. Thoreson,[177] E. Tsai,[177] D. Wood,[177] S. Dittmer,[178] K. A. Hahn,[178] Y. Liu,[178] M. Mcginnis,[178] Y. Miao,[178] D. G. Monk,[178] M. H. Schmitt,[178] A. Taliercio,[178] M. Velasco,[178] J. Wang,[178] G. Agarwal,[179] R. Band,[179] R. Bucci,[179] S. Castells,[179] A. Das,[179] A. Ehnis,[179] R. Goldouzian,[179] M. Hildreth,[179] K. Hurtado Anampa,[179] T. Ivanov,[179] C. Jessop,[179] A. Karneyeu,[179] K. Lannon,[179] J. Lawrence,[179] N. Loukas,[179] L. Lutton,[179] J. Mariano,[179] N. Marinelli,[179] I. Mcalister,[179] T. McCauley,[179] C. Mcgrady,[179] C. Moore,[179] Y. Musienko,[179,oooo] H. Nelson,[179] M. Osherson,[179] A. Piccinelli,[179] R. Ruchti,[179] A. Townsend,[179] Y. Wan,[179] M. Wayne,[179] H. Yockey,[179] A. Basnet,[180] M. Carrigan,[180] R. De Los Santos,[180] L. S. Durkin,[180] C. Hill,[180] M. Joyce,[180] M. Nunez Ornelas,[180] D. A. Wenzl,[180] B. L. Winer,[180] B. R. Yates,[180] H. Bouchamaoui,[181] K. Coldham,[181] P. Das,[181] G. Dezoort,[181] P. Elmer,[181] A. Frankenthal,[181] M. Galli,[181] B. Greenberg,[181] N. Haubrich,[181] K. Kennedy,[181] G. Kopp,[181] Y. Lai,[181] D. Lange,[181] A. Loeliger,[181] D. Marlow,[181] I. Ojalvo,[181] J. Olsen,[181] F. Simpson,[181] D. Stickland,[181] C. Tully,[181] S. Malik,[182] R. Sharma,[182] S. Chandra,[183] R. Chawla,[183] A. Gu,[183] L. Gutay,[183] M. Jones,[183] A. W. Jung,[183] D. Kondratyev,[183] M. Liu,[183] G. Negro,[183] N. Neumeister,[183] G. Paspalaki,[183] S. Piperov,[183] N. R. Saha,[183] J. F. Schulte,[183] F. Wang,[183] A. Wildridge,[183] W. Xie,[183] Y. Yao,[183] Y. Zhong,[183] N. Parashar,[184] A. Pathak,[184] E. Shumka,[184] D. Acosta,[185] A. Agrawal,[185] C. Arbour,[185] T. Carnahan,[185] K. M. Ecklund,[185] S. Freed,[185] P. Gardner,[185] F. J. M. Geurts,[185] T. Huang,[185] I. Krommydas,[185] N. Lewis,[185] W. Li,[185] J. Lin,[185] O. Miguel Colin,[185] B. P. Padley,[185] R. Redjimi,[185] J. Rotter,[185] E. Yigitbasi,[185] Y. Zhang,[185] O. Bessidskaia Bylund,[186] A. Bodek,[186] P. de Barbaro,[186,a] R. Demina,[186] A. Garcia-Bellido,[186] H. S. Hare,[186] O. Hindrichs,[186] N. Parmar,[186] P. Parygin,[186,oooo] H. Seo,[186] R. Taus,[186] B. Chiarito,[187] J. P. Chou,[187] S. V. Clark,[187] S. Donnelly,[187] D. Gadkari,[187] Y. Gershtein,[187] E. Halkiadakis,[187] M. Heindl,[187] C. Houghton,[187] D. Jaroslawski,[187] A. Kobert,[187] S. Konstantinou,[187] I. Laflotte,[187] A. Lath,[187] J. Martins,[187] B. Rand,[187] J. Reichert,[187] P. Saha,[187] S. Salur,[187] S. Schnetzer,[187] S. Somalwar,[187] R. Stone,[187] S. A. Thayil,[187] S. Thomas,[187] J. Vora,[187] D. Ally,[188] A. G. Delannoy,[188] S. Fiorendi,[188] J. Harris,[188] S. Higginbotham,[188] T. Holmes,[188] A. R. Kanuganti,[188] N. Karunarathna,[188] J. Lawless,[188] L. Lee,[188] E. Nibigira,[188] B. Skipworth,[188] S. Spanier,[188] D. Aebi,[189] M. Ahmad,[189] T. Akhter,[189] K. Androsov,[189] A. Bolshov,[189] O. Bouhali,[189,pppp] A. Cagnotta,[189] V. D'Amante,[189] R. Eusebi,[189] P. Flanagan,[189] J. Gilmore,[189] Y. Guo,[189] T. Kamon,[189] S. Luo,[189] R. Mueller,[189] A. Safonov,[189] N. Akchurin,[190] J. Damgov,[190] Y. Feng,[190] N. Gogate,[190] Y. Kazhykarim,[190] K. Lamichhane,[190] S. W. Lee,[190] C. Madrid,[190] A. Mankel,[190]

T. Peltola,[190] I. Volobouev,[190] E. Appelt,[191] Y. Chen,[191] S. Greene,[191] A. Gurrola,[191] W. Johns,[191] R. Kunnawalkam Elayavalli,[191] A. Melo,[191] D. Rathjens,[191] F. Romeo,[191] P. Sheldon,[191] S. Tuo,[191] J. Velkovska,[191] J. Viinikainen,[191] J. Zhang,[191] B. Cardwell,[192] H. Chung,[192] B. Cox,[192] J. Hakala,[192] R. Hirosky,[192] M. Jose,[192] A. Ledovskoy,[192] C. Mantilla,[192] C. Neu,[192] C. Ramón Álvarez,[192] S. Bhattacharya,[193] P. E. Karchin,[193] A. Aravind,[194] S. Banerjee,[194] K. Black,[194] T. Bose,[194] E. Chavez,[194] S. Dasu,[194] P. Everaerts,[194] C. Galloni,[194] H. He,[194] M. Herndon,[194] A. Herve,[194] C. K. Koraka,[194] S. Lomte,[194] R. Loveless,[194] A. Mallampalli,[194] A. Mohammadi,[194] S. Mondal,[194] T. Nelson,[194] G. Parida,[194] L. Pétré,[194] D. Pinna,[194] A. Savin,[194] V. Shang,[194] V. Sharma,[194] W. H. Smith,[194] D. Teague,[194] H. F. Tsoi,[194] W. Vetens,[194] A. Warden,[194] S. Afanasiev,[195] V. Alexakhin,[195] Yu. Andreev,[195] T. Aushev,[195] D. Budkouski,[195] R. Chistov,[195,oooo] M. Danilov,[195,oooo] T. Dimova,[195,oooo] A. Ershov,[195,oooo] S. Gninenko,[195] I. Gorbunov,[195] A. Gribushin,[195,oooo] A. Kamenev,[195] V. Karjavine,[195] M. Kirsanov,[195] V. Klyukhin,[195,oooo] O. Kodolova,[195,qqqq,oooo] V. Korenkov,[195] A. Kozyrev,[195,oooo] N. Krasnikov,[195] A. Lanev,[195] A. Malakhov,[195] V. Matveev,[195,oooo] A. Nikitenko,[195,rrrr,qqqq] V. Palichik,[195] V. Perelygin,[195] S. Petrushanko,[195,oooo] S. Polikarpov,[195,oooo] O. Radchenko,[195,oooo] M. Savina,[195] V. Shalaev,[195] S. Shmatov,[195] S. Shulha,[195] Y. Skovpen,[195,oooo] V. Smirnov,[195] O. Teryaev,[195] I. Tlisova,[195,oooo] A. Toropin,[195] N. Voytishin,[195] B. S. Yuldashev,[195,a,ssss] A. Zarubin,[195] I. Zhizhin,[195] L. Dudko,[196] K. Ivanov,[196] V. Kim,[196,oooo] V. Murzin,[196] V. Oreshkin,[196] D. Sosnov,[196] E. Boos,[196] V. Bunichev,[196] M. Dubinin,[196,hhhh] V. Savrin,[196] and A. Snigirev[196]

(CMS Collaboration)

[1]*Yerevan Physics Institute, Yerevan, Armenia*
[2]*Institut für Hochenergiephysik, Vienna, Austria*
[3]*Universiteit Antwerpen, Antwerpen, Belgium*
[4]*Vrije Universiteit Brussel, Brussel, Belgium*
[5]*Université Libre de Bruxelles, Bruxelles, Belgium*
[6]*Ghent University, Ghent, Belgium*
[7]*Université Catholique de Louvain, Louvain-la-Neuve, Belgium*
[8]*Centro Brasileiro de Pesquisas Fisicas, Rio de Janeiro, Brazil*
[9]*Universidade do Estado do Rio de Janeiro, Rio de Janeiro, Brazil*
[10]*Universidade Estadual Paulista, Universidade Federal do ABC, São Paulo, Brazil*
[11]*Institute for Nuclear Research and Nuclear Energy, Bulgarian Academy of Sciences, Sofia, Bulgaria*
[12]*University of Sofia, Sofia, Bulgaria*
[13]*Instituto De Alta Investigación, Universidad de Tarapacá, Casilla 7 D, Arica, Chile*
[14]*Universidad Tecnica Federico Santa Maria, Valparaiso, Chile*
[15]*Beihang University, Beijing, China*
[16]*Department of Physics, Tsinghua University, Beijing, China*
[17]*Institute of High Energy Physics, Beijing, China*
[18]*State Key Laboratory of Nuclear Physics and Technology, Peking University, Beijing, China*
[19]*State Key Laboratory of Nuclear Physics and Technology, Institute of Quantum Matter, South China Normal University, Guangzhou, China*
[20]*Sun Yat-Sen University, Guangzhou, China*
[21]*University of Science and Technology of China, Hefei, China*
[22]*Nanjing Normal University, Nanjing, China*
[23]*Institute of Modern Physics and Key Laboratory of Nuclear Physics and Ion-beam Application (MOE)—Fudan University, Shanghai, China*
[24]*Zhejiang University, Hangzhou, Zhejiang, China*
[25]*Universidad de Los Andes, Bogota, Colombia*
[26]*Universidad de Antioquia, Medellin, Colombia*
[27]*University of Split, Faculty of Electrical Engineering, Mechanical Engineering and Naval Architecture, Split, Croatia*
[28]*University of Split, Faculty of Science, Split, Croatia*
[29]*Institute Rudjer Boskovic, Zagreb, Croatia*
[30]*University of Cyprus, Nicosia, Cyprus*
[31]*Charles University, Prague, Czech Republic*
[32]*Escuela Politecnica Nacional, Quito, Ecuador*
[33]*Universidad San Francisco de Quito, Quito, Ecuador*

[34]*Academy of Scientific Research and Technology of the Arab Republic of Egypt, Egyptian Network of High Energy Physics, Cairo, Egypt*
[35]*Center for High Energy Physics (CHEP-FU), Fayoum University, El-Fayoum, Egypt*
[36]*National Institute of Chemical Physics and Biophysics, Tallinn, Estonia*
[37]*Department of Physics, University of Helsinki, Helsinki, Finland*
[38]*Helsinki Institute of Physics, Helsinki, Finland*
[39]*Lappeenranta-Lahti University of Technology, Lappeenranta, Finland*
[40]*IRFU, CEA, Université Paris-Saclay, Gif-sur-Yvette, France*
[41]*Laboratoire Leprince-Ringuet, CNRS/IN2P3, Ecole Polytechnique, Institut Polytechnique de Paris, Palaiseau, France*
[42]*Université de Strasbourg, CNRS, IPHC UMR 7178, Strasbourg, France*
[43]*Centre de Calcul de l'Institut National de Physique Nucleaire et de Physique des Particules, CNRS/IN2P3, Villeurbanne, France*
[44]*Institut de Physique des 2 Infinis de Lyon (IP2I), Villeurbanne, France*
[45]*Georgian Technical University, Tbilisi, Georgia*
[46]*RWTH Aachen University, I. Physikalisches Institut, Aachen, Germany*
[47]*RWTH Aachen University, III. Physikalisches Institut A, Aachen, Germany*
[48]*RWTH Aachen University, III. Physikalisches Institut B, Aachen, Germany*
[49]*Deutsches Elektronen-Synchrotron, Hamburg, Germany*
[50]*University of Hamburg, Hamburg, Germany*
[51]*Karlsruher Institut fuer Technologie, Karlsruhe, Germany*
[52]*Institute of Nuclear and Particle Physics (INPP), NCSR Demokritos, Aghia Paraskevi, Greece*
[53]*National and Kapodistrian University of Athens, Athens, Greece*
[54]*National Technical University of Athens, Athens, Greece*
[55]*University of Ioánnina, Ioánnina, Greece*
[56]*HUN-REN Wigner Research Centre for Physics, Budapest, Hungary*
[57]*MTA-ELTE Lendület CMS Particle and Nuclear Physics Group, Eötvös Loránd University, Budapest, Hungary*
[58]*Faculty of Informatics, University of Debrecen, Debrecen, Hungary*
[59]*HUN-REN ATOMKI—Institute of Nuclear Research, Debrecen, Hungary*
[60]*Karoly Robert Campus, MATE Institute of Technology, Gyongyos, Hungary*
[61]*Panjab University, Chandigarh, India*
[62]*University of Delhi, Delhi, India*
[63]*University of Hyderabad, Hyderabad, India*
[64]*Indian Institute of Technology Kanpur, Kanpur, India*
[65]*Saha Institute of Nuclear Physics, HBNI, Kolkata, India*
[66]*Indian Institute of Technology Madras, Madras, India*
[67]*IISER Mohali, India, Mohali, India*
[68]*Tata Institute of Fundamental Research-A, Mumbai, India*
[69]*Tata Institute of Fundamental Research-B, Mumbai, India*
[70]*National Institute of Science Education and Research, An OCC of Homi Bhabha National Institute, Bhubaneswar, Odisha, India*
[71]*Indian Institute of Science Education and Research (IISER), Pune, India*
[72]*Indian Institute of Technology Hyderabad, Telangana, India*
[73]*Isfahan University of Technology, Isfahan, Iran*
[74]*Institute for Research in Fundamental Sciences (IPM), Tehran, Iran*
[75]*University College Dublin, Dublin, Ireland*
[76a]*INFN Sezione di Bari, Bari, Italy*
[76b]*Università di Bari, Bari, Italy*
[76c]*Politecnico di Bari, Bari, Italy*
[77a]*INFN Sezione di Bologna, Bologna, Italy*
[77b]*Università di Bologna, Bologna, Italy*
[78a]*INFN Sezione di Catania, Catania, Italy*
[78b]*Università di Catania, Catania, Italy*
[79a]*INFN Sezione di Firenze, Firenze, Italy*
[79b]*Università di Firenze, Firenze, Italy*
[80]*INFN Laboratori Nazionali di Frascati, Frascati, Italy*
[81a]*INFN Sezione di Genova, Genova, Italy*
[81b]*Università di Genova, Genova, Italy*
[82a]*INFN Sezione di Milano-Bicocca, Milano, Italy*

[82b]*Università di Milano-Bicocca, Milano, Italy*
[83a]*INFN Sezione di Napoli, Napoli, Italy*
[83b]*Università di Napoli 'Federico II', Napoli, Italy*
[83c]*Università della Basilicata, Potenza, Italy*
[83d]*Scuola Superiore Meridionale (SSM), Napoli, Italy*
[84a]*INFN Sezione di Padova, Padova, Italy*
[84b]*Università di Padova, Padova, Italy*
[84c]*Universita degli Studi di Cagliari, Cagliari, Italy*
[85a]*INFN Sezione di Pavia, Pavia, Italy*
[85b]*Università di Pavia, Pavia, Italy*
[86a]*INFN Sezione di Perugia, Perugia, Italy*
[86b]*Università di Perugia, Perugia, Italy*
[87a]*INFN Sezione di Pisa, Pisa, Italy*
[87b]*Università di Pisa, Pisa, Italy*
[87c]*Scuola Normale Superiore di Pisa, Pisa, Italy*
[87d]*Università di Siena, Siena, Italy*
[88a]*INFN Sezione di Roma, Roma, Italy*
[88b]*Sapienza Università di Roma, Roma, Italy*
[89a]*INFN Sezione di Torino, Torino, Italy*
[89b]*Università di Torino, Torino, Italy*
[89c]*Università del Piemonte Orientale, Novara, Italy*
[90a]*INFN Sezione di Trieste, Trieste, Italy*
[90b]*Università di Trieste, Trieste, Italy*
[91]*Kyungpook National University, Daegu, Korea*
[92]*Department of Mathematics and Physics—GWNU, Gangneung, Korea*
[93]*Chonnam National University, Institute for Universe and Elementary Particles, Kwangju, Korea*
[94]*Hanyang University, Seoul, Korea*
[95]*Korea University, Seoul, Korea*
[96]*Kyung Hee University, Department of Physics, Seoul, Korea*
[97]*Sejong University, Seoul, Korea*
[98]*Seoul National University, Seoul, Korea*
[99]*University of Seoul, Seoul, Korea*
[100]*Yonsei University, Department of Physics, Seoul, Korea*
[101]*Sungkyunkwan University, Suwon, Korea*
[102]*College of Engineering and Technology, American University of the Middle East (AUM), Dasman, Kuwait*
[103]*Kuwait University—College of Science—Department of Physics, Safat, Kuwait*
[104]*Riga Technical University, Riga, Latvia*
[105]*University of Latvia (LU), Riga, Latvia*
[106]*Vilnius University, Vilnius, Lithuania*
[107]*National Centre for Particle Physics, Universiti Malaya, Kuala Lumpur, Malaysia*
[108]*Universidad de Sonora (UNISON), Hermosillo, Mexico*
[109]*Centro de Investigacion y de Estudios Avanzados del IPN, Mexico City, Mexico*
[110]*Universidad Iberoamericana, Mexico City, Mexico*
[111]*Benemerita Universidad Autonoma de Puebla, Puebla, Mexico*
[112]*University of Montenegro, Podgorica, Montenegro*
[113]*University of Canterbury, Christchurch, New Zealand*
[114]*National Centre for Physics, Quaid-I-Azam University, Islamabad, Pakistan*
[115]*AGH University of Krakow, Krakow, Poland*
[116]*National Centre for Nuclear Research, Swierk, Poland*
[117]*Institute of Experimental Physics, Faculty of Physics, University of Warsaw, Warsaw, Poland*
[118]*Warsaw University of Technology, Warsaw, Poland*
[119]*Laboratório de Instrumentação e Física Experimental de Partículas, Lisboa, Portugal*
[120]*Faculty of Physics, University of Belgrade, Belgrade, Serbia*
[121]*VINCA Institute of Nuclear Sciences, University of Belgrade, Belgrade, Serbia*
[122]*Centro de Investigaciones Energéticas Medioambientales y Tecnológicas (CIEMAT), Madrid, Spain*
[123]*Universidad Autónoma de Madrid, Madrid, Spain*
[124]*Universidad de Oviedo, Instituto Universitario de Ciencias y Tecnologías Espaciales de Asturias (ICTEA), Oviedo, Spain*
[125]*Instituto de Física de Cantabria (IFCA), CSIC-Universidad de Cantabria, Santander, Spain*

[126]*University of Colombo, Colombo, Sri Lanka*
[127]*University of Ruhuna, Department of Physics, Matara, Sri Lanka*
[128]*CERN, European Organization for Nuclear Research, Geneva, Switzerland*
[129]*PSI Center for Neutron and Muon Sciences, Villigen, Switzerland*
[130]*ETH Zurich—Institute for Particle Physics and Astrophysics (IPA), Zurich, Switzerland*
[131]*Universität Zürich, Zurich, Switzerland*
[132]*National Central University, Chung-Li, Taiwan*
[133]*National Taiwan University (NTU), Taipei, Taiwan*
[134]*High Energy Physics Research Unit, Department of Physics, Faculty of Science, Chulalongkorn University, Bangkok, Thailand*
[135]*Tunis El Manar University, Tunis, Tunisia*
[136]*Çukurova University, Physics Department, Science and Art Faculty, Adana, Turkey*
[137]*Middle East Technical University, Physics Department, Ankara, Turkey*
[138]*Bogazici University, Istanbul, Turkey*
[139]*Istanbul Technical University, Istanbul, Turkey*
[140]*Istanbul University, Istanbul, Turkey*
[141]*Yildiz Technical University, Istanbul, Turkey*
[142]*Institute for Scintillation Materials of National Academy of Science of Ukraine, Kharkiv, Ukraine*
[143]*National Science Centre, Kharkiv Institute of Physics and Technology, Kharkiv, Ukraine*
[144]*University of Bristol, Bristol, United Kingdom*
[145]*Rutherford Appleton Laboratory, Didcot, United Kingdom*
[146]*Imperial College, London, United Kingdom*
[147]*Brunel University, Uxbridge, United Kingdom*
[148]*Baylor University, Waco, Texas, USA*
[149]*Bethel University, St. Paul, Minnesota, USA*
[150]*Catholic University of America, Washington, DC, USA*
[151]*The University of Alabama, Tuscaloosa, Alabama, USA*
[152]*Boston University, Boston, Massachusetts, USA*
[153]*Brown University, Providence, Rhode Island, USA*
[154]*University of California, Davis, Davis, California, USA*
[155]*University of California, Los Angeles, California, USA*
[156]*University of California, Riverside, Riverside, California, USA*
[157]*University of California, San Diego, La Jolla, California, USA*
[158]*University of California, Santa Barbara—Department of Physics, Santa Barbara, California, USA*
[159]*California Institute of Technology, Pasadena, California, USA*
[160]*Carnegie Mellon University, Pittsburgh, Pennsylvania, USA*
[161]*University of Colorado Boulder, Boulder, Colorado, USA*
[162]*Cornell University, Ithaca, New York, USA*
[163]*Fermi National Accelerator Laboratory, Batavia, Illinois, USA*
[164]*University of Florida, Gainesville, Florida, USA*
[165]*Florida State University, Tallahassee, Florida, USA*
[166]*Florida Institute of Technology, Melbourne, Florida, USA*
[167]*University of Illinois Chicago, Chicago, Illinois, USA*
[168]*The University of Iowa, Iowa City, Iowa, USA*
[169]*Johns Hopkins University, Baltimore, Maryland, USA*
[170]*The University of Kansas, Lawrence, Kansas, USA*
[171]*Kansas State University, Manhattan, Kansas, USA*
[172]*University of Maryland, College Park, Maryland, USA*
[173]*Massachusetts Institute of Technology, Cambridge, Massachusetts, USA*
[174]*University of Minnesota, Minneapolis, Minnesota, USA*
[175]*University of Nebraska-Lincoln, Lincoln, Nebraska, USA*
[176]*State University of New York at Buffalo, Buffalo, New York, USA*
[177]*Northeastern University, Boston, Massachusetts, USA*
[178]*Northwestern University, Evanston, Illinois, USA*
[179]*University of Notre Dame, Notre Dame, Indiana, USA*
[180]*The Ohio State University, Columbus, Ohio, USA*
[181]*Princeton University, Princeton, New Jersey, USA*
[182]*University of Puerto Rico, Mayaguez, Puerto Rico, USA*
[183]*Purdue University, West Lafayette, Indiana, USA*
[184]*Purdue University Northwest, Hammond, Indiana, USA*

[185]*Rice University, Houston, Texas, USA*
[186]*University of Rochester, Rochester, New York, USA*
[187]*Rutgers, The State University of New Jersey, Piscataway, New Jersey, USA*
[188]*University of Tennessee, Knoxville, Tennessee, USA*
[189]*Texas A&M University, College Station, Texas, USA*
[190]*Texas Tech University, Lubbock, Texas, USA*
[191]*Vanderbilt University, Nashville, Tennessee, USA*
[192]*University of Virginia, Charlottesville, Virginia, USA*
[193]*Wayne State University, Detroit, Michigan, USA*
[194]*University of Wisconsin—Madison, Madison, Wisconsin, USA*
[195]*An institute or international laboratory covered by a cooperation agreement with CERN*
[196]*An institute formerly covered by a cooperation agreement with CERN*

[a]Deceased.
[b]Also at Yerevan State University, Yerevan, Armenia.
[c]Also at TU Wien, Vienna, Austria.
[d]Also at Ghent University, Ghent, Belgium.
[e]Also at Universidade do Estado do Rio de Janeiro, Rio de Janeiro, Brazil.
[f]Also at FACAMP—Faculdades de Campinas, Sao Paulo, Brazil.
[g]Also at Universidade Estadual de Campinas, Campinas, Brazil.
[h]Also at Federal University of Rio Grande do Sul, Porto Alegre, Brazil.
[i]Also at The University of the State of Amazonas, Manaus, Brazil.
[j]Also at University of Chinese Academy of Sciences, Beijing, China.
[k]Also at China Center of Advanced Science and Technology, Beijing, China.
[l]Also at University of Chinese Academy of Sciences, Beijing, China.
[m]Also at School of Physics, Zhengzhou University, Zhengzhou, China.
[n]Also at Henan Normal University, Xinxiang, China.
[o]Also at University of Shanghai for Science and Technology, Shanghai, China.
[p]Also at The University of Iowa, Iowa City, Iowa, USA.
[q]Also at Center for High Energy Physics, Peking University, Beijing, China.
[r]Also at Helwan University, Cairo, Egypt.
[s]Also at Zewail City of Science and Technology, Zewail, Egypt.
[t]Also at British University in Egypt, Cairo, Egypt.
[u]Also at Purdue University, West Lafayette, Indiana, USA.
[v]Also at Université de Haute Alsace, Mulhouse, France.
[w]Also at Istinye University, Istanbul, Turkey.
[x]Also at Another institute or international laboratory covered by a cooperation agreement with CERN.
[y]Also at University of Hamburg, Hamburg, Germany.
[z]Also at RWTH Aachen University, III. Physikalisches Institut A, Aachen, Germany.
[aa]Also at Bergische University Wuppertal (BUW), Wuppertal, Germany.
[bb]Also at Brandenburg University of Technology, Cottbus, Germany.
[cc]Also at Forschungszentrum Jülich, Juelich, Germany.
[dd]Also at CERN, European Organization for Nuclear Research, Geneva, Switzerland.
[ee]Also at HUN-REN ATOMKI—Institute of Nuclear Research, Debrecen, Hungary.
[ff]Also at Universitatea Babes-Bolyai—Facultatea de Fizica, Cluj-Napoca, Romania.
[gg]Also at MTA-ELTE Lendület CMS Particle and Nuclear Physics Group, Eötvös Loránd University, Budapest, Hungary.
[hh]Also at HUN-REN Wigner Research Centre for Physics, Budapest, Hungary.
[ii]Also at Physics Department, Faculty of Science, Assiut University, Assiut, Egypt.
[jj]Also at The University of Kansas, Lawrence, Kansas, USA.
[kk]Also at Punjab Agricultural University, Ludhiana, India.
[ll]Also at University of Hyderabad, Hyderabad, India.
[mm]Also at Indian Institute of Science (IISc), Bangalore, India.
[nn]Also at University of Visva-Bharati, Santiniketan, India.
[oo]Also at IIT Bhubaneswar, Bhubaneswar, India.
[pp]Also at Institute of Physics, Bhubaneswar, India.
[qq]Also at Deutsches Elektronen-Synchrotron, Hamburg, Germany.
[rr]Also at Isfahan University of Technology, Isfahan, Iran.
[ss]Also at Sharif University of Technology, Tehran, Iran.
[tt]Also at Department of Physics, University of Science and Technology of Mazandaran, Behshahr, Iran.
[uu]Also at Department of Physics, Faculty of Science, Arak University, ARAK, Iran.

[vv]Also at Italian National Agency for New Technologies, Energy and Sustainable Economic Development, Bologna, Italy.
[ww]Also at Centro Siciliano di Fisica Nucleare e di Struttura Della Materia, Catania, Italy.
[xx]Also at James Madison University, Harrisonburg, N/A, USA.
[yy]Also at Università degli Studi Guglielmo Marconi, Roma, Italy.
[zz]Also at Scuola Superiore Meridionale, Università di Napoli 'Federico II', Napoli, Italy.
[aaa]Also at Fermi National Accelerator Laboratory, Batavia, Illinois, USA.
[bbb]Also at Lulea University of Technology, Lulea, Sweden.
[ccc]Also at Consiglio Nazionale delle Ricerche—Istituto Officina dei Materiali, Perugia, Italy.
[ddd]Also at UPES—University of Petroleum and Energy Studies, Dehradun, India.
[eee]Also at Institut de Physique des 2 Infinis de Lyon (IP2I), Villeurbanne, France.
[fff]Also at Department of Applied Physics, Faculty of Science and Technology, Universiti Kebangsaan Malaysia, Bangi, Malaysia.
[ggg]Also at Trincomalee Campus, Eastern University, Sri Lanka, Nilaveli, Sri Lanka.
[hhh]Also at Saegis Campus, Nugegoda, Sri Lanka.
[iii]Also at National and Kapodistrian University of Athens, Athens, Greece.
[jjj]Also at Ecole Polytechnique Fédérale Lausanne, Lausanne, Switzerland.
[kkk]Also at Universität Zürich, Zurich, Switzerland.
[lll]Also at Stefan Meyer Institute for Subatomic Physics, Vienna, Austria.
[mmm]Also at Near East University, Research Center of Experimental Health Science, Mersin, Turkey.
[nnn]Also at Konya Technical University, Konya, Turkey.
[ooo]Also at Izmir Bakircay University, Izmir, Turkey.
[ppp]Also at Adiyaman University, Adiyaman, Turkey.
[qqq]Also at Bozok Universitetesi Rektörlügü, Yozgat, Turkey.
[rrr]Also at Istanbul Sabahattin Zaim University, Istanbul, Turkey.
[sss]Also at Marmara University, Istanbul, Turkey.
[ttt]Also at Milli Savunma University, Istanbul, Turkey.
[uuu]Also at Informatics and Information Security Research Center, Gebze/Kocaeli, Turkey.
[vvv]Also at Kafkas University, Kars, Turkey.
[www]Also at Istanbul Okan University, Istanbul, Turkey.
[xxx]Also at Hacettepe University, Ankara, Turkey.
[yyy]Also at Erzincan Binali Yildirim University, Erzincan, Turkey.
[zzz]Also at Istanbul University—Cerrahpasa, Faculty of Engineering, Istanbul, Turkey.
[aaaa]Also at Yildiz Technical University, Istanbul, Turkey.
[bbbb]Also at School of Physics and Astronomy, University of Southampton, Southampton, United Kingdom.
[cccc]Also at Monash University, Faculty of Science, Clayton, Australia.
[dddd]Also at Bethel University, St. Paul, Minnesota, USA.
[eeee]Also at Università di Torino, Torino, Italy.
[ffff]Also at Karamanoğlu Mehmetbey University, Karaman, Turkey.
[gggg]Also at California Lutheran University;, Thousand Oaks, California, USA.
[hhhh]Also at California Institute of Technology, Pasadena, California, USA.
[iiii]Also at United States Naval Academy, Annapolis, Maryland, USA.
[jjjj]Also at Bingol University, Bingol, Turkey.
[kkkk]Also at Georgian Technical University, Tbilisi, Georgia.
[llll]Also at Sinop University, Sinop, Turkey.
[mmmm]Also at Erciyes University, Kayseri, Turkey.
[nnnn]Also at Horia Hulubei National Institute of Physics and Nuclear Engineering (IFIN-HH), Bucharest, Romania.
[oooo]Also at Another institute formerly covered by a cooperation agreement with CERN.
[pppp]Also at Hamad Bin Khalifa University (HBKU), Doha, Qatar.
[qqqq]Also at Yerevan Physics Institute, Yerevan, Armenia.
[rrrr]Also at Imperial College, London, United Kingdom.
[ssss]Also at Institute of Nuclear Physics of the Uzbekistan Academy of Sciences, Tashkent, Uzbekistan.